# TRANSPORT OF MUONIC ATOMS

by

Edmond Rusjan

Dissertation submitted to the Faculty of the

Virginia Polytechnic Institute and State University

in partial fulfillment of the requirements for the degree

of

DOCTOR OF PHILOSOPHY

in

Mathematical Physics

APPROVED:

_____

P. F. Zweifel, Chairman

_____ _____

W. Greenberg M. Klaus

_____ _____

J. Slawny H. C. Tze

August, 1988

Blacksburg, Virginia

TRANSPORT OF MUONIC ATOMS

by

Edmond Rusjan

Committee Chairman: P. F. Zweifel

Department of Physics

(ABSTRACT)

Transport of muonic hydrogen and deuterium atoms in gaseous hydrogen and deuterium is studied in the diffusion approximation and by means of the multiple collision expansion. The diffusion coefficient is derived. Scattering kernels are computed from the kinematics of an inelastic binary collision. The effect of rotations of the target molecules is treated by defining and computing an effective inelastic energy transfer $Q_{eff}$. The Doppler effect is taken into account by averaging the cross sections over the Maxwellian velocity distribution of the target molecules. Numerical results of the time-dependent problem in slab geometry are presented.

In part two we construct a candidate for a realistic four generation Calabi-Yau manifold by dividing an algebraic variety in $CP_4 \times CP_4$ with the $Z_2 \times Z_2$ symmetry. A nontrivial embedding of $Z_2 \times Z_2$ in E(6) allows the physically interesting intermediate symmetry, based on Pati-Salam $SU(2)_L \times SU(2)_R \times SU(4)_C$ group. The group of honest symmetries $G_H$ of the manifold is identified and the transformations properties of quark and lepton fields under $G_H$ are given.

DEDICATION

to my parents

ACKNOWLEDGEMENTS

First and foremost I would like to thank my advisor Professor Paul F. Zweifel for his guidance and support, advice and encouragement, for being like a father to me. My deepest gratitude goes to Professor Goran Senjanovic, teacher and dearest friend, for all the hours spent together, in research and otherwise.

I would like to thank everybody who helped me with work on the dissertation, especially Professors R. Siegel, S. Paveri-Fontana and C.V.M. van der Mee with the first part and Professors R. Mohapatra, D. Chang, P. Pal and S. Sokorac with the second part. Numerous discussions with them have been both pleasant and fruitful.

For my pleasant stay in Blacksburg and for the education that I received here, I would like to thank my advisory committee, in particular Professors W. Greenberg, J. Slawny, G. Hagedorn, M. Klaus, H. C. Tze, R. L. Bowden and other members of the Center for Transport Theory and Mathematical Physics, especially Mrs. G. Henneke, who provides it with the uniquely pleasant atmosphere. Without her help this work would have never been finished.

Last, but not least, I thank my fellow graduate students and friends in Blacksburg.

TABLE OF CONTENTS

# 1. INTRODUCTION

Transport theory is the study of transport of particles or energy, generally through a host medium. The origins go back more than a century ago, when Boltzmann developed the kinetic theory of gases[1]. Methods for solving the transport equations were first developed during the thirties to analyze problems in radiative transfer[2]. In the fifties and the sixties there was an enormous amount of research in neutron transport theory motivated by the nuclear energy program[3]. At first, these disciplines developed to a large degree independently. As the subject matured, however, more emphasis was given to unifying the various approaches used in different fields and to providing a firm mathematical footing for the techniques used in solving the transport equations[4-6]. This yielded to the study of transport problems in an abstract mathematical setting[7-9]. Many excellent books now cover the subject as a whole, as well as various specialized topics[2,3,10-15].

The above mentioned kinetic theory, radiative transfer and neutron transport theory are not the only applications of transport theory. Others include transport of charged particles, plasma physics, scattering of radar waves from atmospheric turbulence and transport in biological systems. New applications are still being found, such as transport of muonic atoms, which we study in this work. As we shall see, transport of muonic atoms is in many respects similar to neutron transport, but it also exhibits some characteristic and interesting features.

We shall primarily be interested in hydrogen (and deuterium) muonic atoms. These are simply ordinary hydrogen atoms, with the electron replaced by a muon. They are neutral and very small (Bohr radius

approximately 250 fm) and hence they behave similarly to neutrons. As ordinary hydrogen atoms, muonic hydrogen atoms can also exist in triplet state (proton and muon spin parallel, i.e. S = 1) and in singlet state (spins antiparallel, i.e. S = 0). In a collision with a molecule muonic atoms can be excited and de-excited between these two states. Also, the singlet-singlet scattering cross section is different from the triplet-triplet case, so it is essential to distinguish between the singlet and triplet states during the diffusion process. The hyperfine splitting between the two hyperfine states in ordinary hydrogen has an energy of only $5.9 \times 10^{-6}$ eV, which is the well-known 21 cm line used in radioastronomy. The hyperfine splitting in muonic hydrogen is bigger than in ordinary hydrogen by a factor of (muon mass/electron mass)$^2$ and is about 0.183 eV. Since the kinetic energies of muonic atoms considered in this work are of the same order of magnitude, the inelasticity of the singlet-triplet transitions must be taken into account in the diffusion process.

An understanding of the diffusion of muonic hydrogen and/or deuterium atoms in molecular hydrogen and/or deuterium is needed for the analysis of experiments on nuclear capture of muons[16,17]. Even more important is the application to the study of muon catalyzed fusion. This process, in which a muon catalyzes a fusion of two hydrogen isotopes, was first predicted in 1947[18] and was discovered experimentally ten years later[19]. What happens is that in a muonic hydrogen molecule the nuclei are separated by only about 250 fm and fusion is possible due to quantum-mechanical tunneling through the Coulomb barrier. In fact a deuterium-deuterium and deuterium-tritium molecule formation leads in

almost all cases to fusion. The muon survives the fusion reaction and, if it does not get stuck to the helium nucleus, it can catalyze another fusion reaction, and so on. The possibility of using this process for energy purposes is being seriously considered[20-24].

As we have mentioned, muonic hydrogen atoms behave similarly to neutrons, so it is quite reasonable to use methods of neutron transport theory. The diffusion process, which we study, is governed by a system of two coupled (one for singlet, one for triplet state) time, space and energy dependent linear transport equations, whose solution is intractable unless certain simplifying assumptions are made. We develop a method for treating this transport, which is basically a modified time dependent diffusion theory, similar to the Selengut-Goertzel method[14] developed in the 1950's for treating neutron transport in $H_2O$ reactors. In Sec. 2 we show how the diffusion approximation is obtained from the transport equation and in particular derive an expression for the diffusion coefficient, which in the muonic case is a matrix. We study the problem in infinite slab geometry, which is an excellent model of the actual experimental setup, used by Professor Siegel and his group in their muonic atom diffusion experiments[25].

The parameters in the diffusion equation are certain scattering kernels and scattering angles. The well-known formulas for these quantities from the neutron transport theory[11,13] do not apply directly in the muonic case. They need to be generalized due to the inelasticity of S→T and T→S transitions. In Sec. 3 we derive them for the case of a medium at zero temperature. In analogy with the elastic case[11], this is obtained from the study of the kinematics (inelastic) of the muonic

atom colliding with a stationary scattering center. The inelasticity of the S→T and T→S collisions is slightly modified by induced rotational transitions in the target, which are required to conserve angular momentum. In Sec. 4 we compute the change in the hyperfine transition energy taking into account the rotational energy levels of the scatterer (i.e. a hydrogen molecule). Vibrational transitions are ignored, because of their high energy. The changes induced in the scattering kernels and scattering angles by the thermal motion of the molecules (Doppler effect) are described in Sec. 5. They are obtained by averaging the zero temperature formulas over the Maxwellian velocity distribution of the target molecules.

The accuracy of the diffusion approximation can be improved considerably by separating the uncollided flux, which is computed analytically in Sec. 6. Then the diffusion equation is solved (numerically) for the collided flux. The numerics are briefly described in Sec. 7. All calculations are done in slab geometry. For the sake of clarity, the calculations do not take into account the finite lifetime of the muon ($\tau_\mu = 2\mu s$), since it is independent of the scattering process and its effect can be included by multiplying all the results by the factor $\exp(-t/\tau_\mu)$. The numerical computations were carried out on the CRAY XM-P at the Pittsburgh computer center. In Sec. 8, we present results for a number of initial source energies and a number of temperatures for both muonic hydrogen and deuterium atoms diffusing in molecular hydrogen and deuterium, respectively.

Some of the results, in particular the prediction of the bump on the emerging flux curve, seemed surprising, when they were first obtained.

In order to confirm them and gain a better understanding, we developed the one-speed model of Sec. 9.

Diffusion approximation is only applicable to optically thick media, i.e. to geometries whose characteristic dimensions are much larger than the mean free path. On the other hand, a number of experiments have been performed in optically thin systems[25]. For such systems we suggest a multiple collison expansion[26,27], which we have implemented to low order. In Sec. 10, we present this approximation, together with the results, which compare favorably with experiments.

The numerical codes, used in solving the diffusion equation, in the multiple collision expansion and in calculating the change in inelasticity of the singlet-triplet and triplet-singlet collisions due to the rotations of the target molecules, are given in the Appendix, together with a short description.

## 2. DERIVATION OF THE DIFFUSION EQUATION

The muonic hydrogen atoms can exist in two hyperfine states, namely in singlet and triplet (doublet and quartet in the case of deuterium). Since, as always in transport theory, we are not interested in the fate of each individual atom, we adopt the statistical description, i.e. we define the angular density for the singlet state (and similarly for the triplet state) by

$$\psi_S(t,x\,\mu,E)\;dx\;d\mu\;dE \;=\; \#\text{ of singlet atoms that are at time t in the interval } dx\;d\mu\;dE \text{ about } (x,\mu,E), \qquad (2.1)$$

where x is position, $\mu$ the cosine of the angle between the velocity and the x-axis and E the energy. We assume the muonic atoms to be diffusing in an infinite slab of thickness d. The notation is standard [3]. We see that the angular density is a two component vector and so is the angular flux:

$$\Phi(t,x,\mu,E) \;=\; \begin{bmatrix} \phi_S(t,x,\mu,E) \\ \phi_T(t,x,\mu,E) \end{bmatrix} \;=\; v \begin{bmatrix} \psi_S(t,x,\mu,E) \\ \psi_S(t,x,\mu,E) \end{bmatrix} \quad . \qquad (2.2)$$

Here v is the speed of the muonic atom ( = $(2E/m)^{1/2}$ ).

$\Phi$ obeys a linear Boltzmann equation, formally identical to the neutron transport equation [3],

$$\frac{1}{v}\frac{\partial\Phi(t,x,\mu,E)}{\partial t} + \mu\frac{\partial\Phi}{\partial x} + \Sigma(E)\Phi = \int \Sigma(E',\mu'\text{->}E,\mu)\Phi(t,x,\mu',E')d\mu'dE' \;, \qquad (2.3)$$

but in the muonic case the total cross section $\Sigma(E)$ and the scattering kernel $\Sigma(E',\mu'\rightarrow E,\mu)$ are matrices. The total cross section is diagonal:

$$\Sigma(E) = \begin{bmatrix} \Sigma_S(E) & 0 \\ 0 & \Sigma_T(E) \end{bmatrix} , \qquad (2.4)$$

where $\Sigma_S(E)$ (respectively $\Sigma_T(E)$) is the total cross section for scattering of singlet (respectively triplet) muonic atoms. The scattering kernel $\Sigma(E',\mu'->E,\mu) = \Sigma(E'->E,\mu_0)$, where $\mu_0$ is the cosine of the scattering angle, can be written as

$$\Sigma(E',\mu'->E,\mu) = \begin{bmatrix} \Sigma_{SS}(E',\mu'->E,\mu) & \Sigma_{TS}(E',\mu'->E,\mu) \\ \Sigma_{ST}(E',\mu'->E,\mu) & \Sigma_{TT}(E',\mu'->E,\mu) \end{bmatrix} . \qquad (2.5)$$

Here $\Sigma_{ab}$ is the scattering cross section for an atom in the spin state a to scatter to spin state b. The total cross sections of Eq.(2.4) are related to those of Eq.(2.5) by

$$\Sigma_a(E') = \int dE\, d\mu \, ( \Sigma_{aa}(E',\mu'->E,\mu) + \Sigma_{ab}(E',\mu'->E,\mu) ) . \qquad (2.6)$$

To develop a diffusion theory, the standard procedure is to expand the angular flux in a series of Legendre polynomials and retain only the first two terms:

$$\Phi(t,x,\mu,E) = \frac{1}{2} \Phi_0(t,x,E) + \frac{3}{2} \mu \Phi_1(t,x,E) , \qquad (2.7)$$

where $\Phi_0$ is the total flux (or simply the flux) and $\Phi_1$ the current. We obtain the following equations, known in neutron transport theory as the P-1 approximation [14]

$$\frac{1}{v} \frac{\partial \Phi_0(t,x,E)}{\partial t} + \frac{\partial \Phi_1}{\partial x} + \Sigma(E)\Phi_0 = \int \Sigma_0(E'->E)\, \Phi_0(t,x,E')\, dE' \qquad (2.8a)$$

$$\frac{1}{v} \frac{\partial \Phi_1(t,x,E)}{\partial t} + \frac{1}{3} \frac{\partial \Phi_0}{\partial x} + \Sigma(E)\Phi_1 = \int \Sigma_1(E'->E)\, \Phi_1(t,x,E')\, dE' . \qquad (2.8b)$$

The kernels $\Sigma_0(E'\text{->}E)$ and $\Sigma_1(E'\text{->}E)$ are the zeroth and the first moments of the scattering kernel $\Sigma(E'\text{->}E,\mu_0)$,

$$\Sigma_i(E'\text{->}E) = \int \Sigma(E'\text{->}E,\mu_0)\ \mu_0^i\ d\mu_0 \quad , \quad i = 0,1. \tag{2.9}$$

The expression for $\Sigma_0(E'\text{->}E)$ is derived in Sec.3-5. In the spirit of the Selengut-Goertzel approximation [14], we set

$$\int \Sigma_1(E'\text{->}E)\ \phi_1(E')\ dE' \approx \begin{bmatrix} \Sigma_{SS}(E)\ \bar{\mu}_{0SS}(E) & \Sigma_{TS}(E)\ \bar{\mu}_{0TS}(E) \\ \Sigma_{ST}(E)\ \bar{\mu}_{0ST}(E) & \Sigma_{TT}(E)\ \bar{\mu}_{0TT}(E) \end{bmatrix} \Phi_1(E) \tag{2.10}$$

where the average cosine of the scattering angle for scattering from spin state a to spin state b, $\bar{\mu}_{0ab}(E)$, is also derived in Sec.3-5. Also, as is customary in diffusion theory, the term $\partial\Phi_1/\partial t$ is neglected.

We thus arrive at the diffusion equation

$$\frac{1}{v}\frac{\partial\Phi_0}{\partial t} - D\frac{\partial^2\Phi_0}{\partial x^2} + \Sigma(E)\Phi_0 = \int \Sigma_0(E'\text{->}E)\ \Phi_0(t,x,E')\ dE' \ , \tag{2.11}$$

where the diffusion matrix D is given by

$$D = \frac{M}{3\ \det M} \quad , \tag{2.12a}$$

$$M = \begin{bmatrix} \Sigma_T - \Sigma_{TT}\ \bar{\mu}_{0TT} & \Sigma_{TS}\ \bar{\mu}_{0TS} \\ \Sigma_{ST}\ \bar{\mu}_{0ST} & \Sigma_S - \Sigma_{SS}\ \bar{\mu}_{0SS} \end{bmatrix} . \tag{2.12b}$$

The boundary condition for the angular flux is, of course, the normal non-reentrant condition at $x = \pm d/2$:

$$\Phi(t,-\frac{d}{2},\mu>0,E) = \Phi(t,\frac{d}{2},\mu<0,E) = 0 \quad . \tag{2.13}$$

In the diffusion approximation this condition cannot be satisfied exactly, but only approximately. We adopt the usual extrapolated - endpoint condition [3,11].

$$\Phi_0(\pm d') = 0 \quad , \tag{2.14a}$$

where the extrapolated endpoint d' is defined by

$$d' = \frac{1}{2}\, d + .7\, \frac{1}{\Sigma_a(E)\ (1-\bar{\mu}_{0aa})} \quad , \quad a = S,T. \tag{2.14b}$$

We see that there is some ambiguity because the extrapolated endpoint is a function of energy and furthermore it is different for the singlet and triplet case. We use an average which should be a good approximation for thick slabs, where the second term in Eq.(2.14b) is a small correction. The restriction to optically thick slabs is necessary for the validity of diffusion theory anyway.

The x-dependence is treated by Fourier expansion

$$\Phi_0(t,x,E) = \sum_{n=1}^{\infty} \Phi_{0n}(t,E)\, \cos(B_n x) \quad , \tag{2.15}$$

where

$$B_n = \frac{(2n-1)\ \pi}{2\ d'} \quad . \tag{2.16}$$

Eq.(2.11) then yields

$$\frac{1}{v}\, \frac{\partial \Phi_{0n}(t,E)}{\partial t} + (D(E)B_n^2 + \Sigma(E))\ \Phi_{0n} = \int \Sigma_0(E'\text{->}E)\ \Phi_{0n}(t,x,E')\ dE' \quad . \tag{2.17}$$

## 3. KINEMATICS

The kinematics of elastic scattering has been studied extensively [28,29]. For the inelastic case Schiff suggests that the kinematics can be obtained from the elastic case by replacing $m_1/m_2$ ($m_1$ = mass of the projectile, $m_2$ = mass of the target) by

$$\gamma = \frac{m_1}{m_2} \left( \frac{E''}{E'' + Q} \right)^{1/2} , \tag{3.1}$$

where $E'' = E' m_1 m_2/(m_1+m_2)$ is the kinetic energy of the scatterer in the center of mass coordinate system and Q is the amount of energy that is converted from internal energy to kinetic energy during the collision process (Q is positive for exothermic and negative for endothermic collisions). This substitution only partially carries out the conversion from elastic to inelastic kinematics. A complete description of the kinematics of inelastic scattering must be derived from conservation of energy and momentum, as in the elastic case [11].

Since only the ratio of the projectile and the target masses is relevant for the kinematics, we may consider a projectile of unit mass and a target of mass A. It is helpful to describe the collision in both the center of mass coordinate system (CMCS) and and in the laboratory coordinate system (LCS). In LCS (resp. CMCS), the projectile enters the collision with speed $v'=(2E')^{1/2}$ (resp. u'), scatters through the angle $\cos^{-1}\mu_0$ (resp. $\cos^{-1}\mu_c$) and emerges with speed $v=(2E)^{1/2}$ (resp. u). Since the CMCS moves relatively to the LCS with speed $v_M=v'/(A+1)$, the speed of the target in the CMCS equals $v_M$ before the collision and is denoted by $v_T$ after the collision. Since the total momentum in the CMCS

equals 0, we have

$$u = A\, v_T \quad . \tag{3.2}$$

Let $V_i$ and $V_f$ be the potential energy of the projectile (in this case, $V_i$ and $V_f$ refer to the internal energies of the triplet and singlet spin states) before and after scattering, respectively. Energy conservation in the CMCS yields

$$\frac{1}{2}(v'-v_M)^2 + V_i + \frac{1}{2} A\, v_M^2 = \frac{1}{2} u^2 + V_f + \frac{1}{2} A\, v_T^2 \quad . \tag{3.3}$$

Combining conservation laws (3.2) and (3.3) and noting that

$$Q = V_i - V_f \quad , \tag{3.4}$$

we find

$$u = \frac{A}{A+1} \beta(E')\, v' \quad , \tag{3.5}$$

where

$$\beta(E') = \left( 1 + \frac{A+1}{A} \frac{Q}{E'} \right)^{1/2} \quad . \tag{3.6}$$

The velocity of the projectile in the LCS is the vector sum of its velocity in the CMCS and the velocity of the CMCS relative to the LCS (Fig.1). Using the law of cosines along with Eq.(3.5) yields immediately

$$\mu_0 = \frac{1 + A\beta\mu_c}{\left( 1 + 2A\beta\mu_c + A^2\beta^2 \right)^{1/2}} \tag{3.7}$$

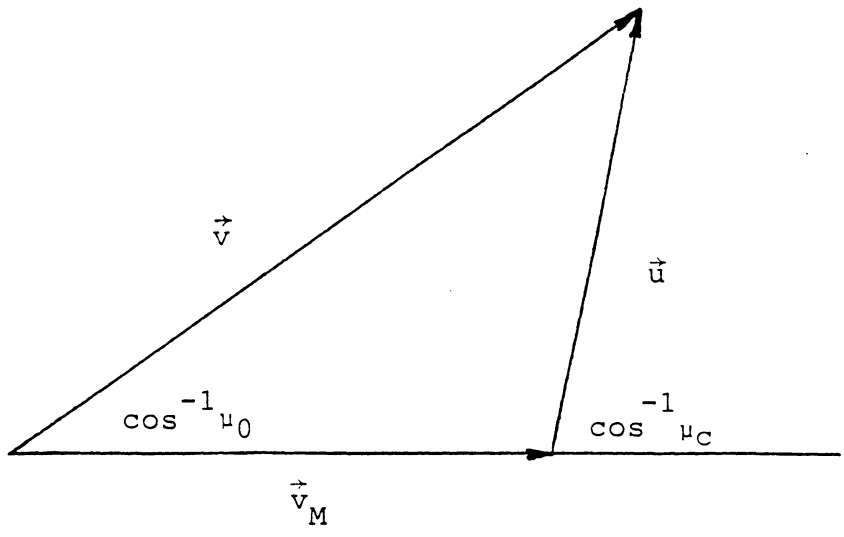


Fig.1 Relation between the LCS and the CMCS velocities.

and a relation between the initial and final energy of the projectile in the LCS as a function of the scattering angle:

$$\frac{E}{E'} = \frac{1}{(A+1)^2} \left( A^2\beta^2 + 2A\beta\mu_c + 1 \right) . \tag{3.8}$$

As $\beta$->1 these reduce to the well-known equation for elastic scattering [11]. At a fixed initial projectile energy E' the scattering angle in the LCS becomes a function of the final projectile energy E

$$\mu_0(E) = \frac{1}{2} \left[ (A+1) \left( \frac{E}{E'} \right)^{1/2} - \frac{A^2\beta^2-1}{A+1} \left( \frac{E'}{E} \right)^{1/2} \right] , \tag{3.9}$$

as follows easily from (3.7) and (3.8).

Now we are ready to use the above relations in computing the scattering cross sections. Because of the low kinetic energy of the projectile, only s-wave (i.e. zero angular momentum) scattering is possible. Therefore the scattering is isotropic in the CMCS:

$$\Sigma(E',\mu_c) = \frac{1}{2} \Sigma(E') . \tag{3.10}$$

From

$$\Sigma(E',\mu_c) \left| d\mu_c \right| = \Sigma(E'\text{->}E) \left| dE \right| \tag{3.11}$$

and equation (3.8) follows

$$\Sigma(E'\text{->}E,\mu_0) = \begin{cases} \frac{(A+1)^2\Sigma(E')}{4AE'\ \beta(E')} \delta(\mu_0 - \mu_0(E)) & \text{if } E^- < E < E^+ \\ 0 & \text{else} \end{cases} , \tag{3.12}$$

where

$$E^{\pm} = E' \frac{(A\beta(E') \pm 1)^2}{(A+1)^2} \quad . \tag{3.13}$$

The delta function in Eq.(3.12) implements the fact that $\mu_0$ is uniquely determined with the choice of E' and E. The moments of the scattering kernel are obtained from (3.12) by a trivial integration. We only need the $0^{th}$ moment

$$\Sigma_0(E'->E) = \begin{cases} \frac{(A+1)^2 \Sigma(E')}{4AE'\ \beta(E')} & \text{if } E^- < E < E^+ \\ 0 & \text{else} \end{cases} \tag{3.14}$$

and the $1^{st}$ moment

$$\Sigma_1(E'->E) = \Sigma_0(E'->E)\ \mu_0(E) \quad . \tag{3.15}$$

The average cosine of the scattering angle in the LCS is obtained by integrating Eq.(3.15) over the final energy:

$$\bar{\mu}_0(E') = \begin{cases} 1 - \frac{1}{2} A\beta(E') + \frac{1}{6} A^2\beta^2(E') & \text{if } Q < 0 \text{ and } E' < \frac{A(-Q)}{A-1} \\ \frac{2}{3\ A\ \beta(E')} & \text{otherwise .} \end{cases} \tag{3.16}$$

Again, the well known elastic limits of the above formulas [11] are recovered by noting that $\beta$->1 as Q->0.

## 4. EFFECTIVE INELASTIC ENERGY TRANSFER ($Q_{eff}$)

In this section we analyze the inelastic processes S->T and T->S more fully. The first argument involves conservation of angular momentum. Because of the very low energy there is no orbital angular momentum involved. Furthermore, radiationless transitions, when allowed, are favoured over photon emission by a factor of $\alpha^2$ ($\alpha$ is the fine structure constant). Therefore, the change in the spin of the atom must be compensated by a change in the angular momentum of the molecule. Let I denote the nuclear spin (I=0 corresponds to parahydrogen, I=1 to orthohydrogen), J the rotational angular momentum of the hydrogen molecule and K their sum. The Pauli principle implies that orthohydrogen is always in an odd J state and parahydrogen in an even J state.

We denote by $W_i$ and $W_f$ the initial and final rotational energy levels of the molecule and write the conservation of energy in the LCS:

$$E' + V_i + W_i = E + V_f + W_f \quad , \tag{4.1}$$

where, we recall, $V_i$ and $V_f$ are the internal energies of the muonic atom. We notice that for the purposes of kinematics V and W play equivalent roles. Hence the proper generalization of the definition of energy transfer Q (Eq.3.4) is

$$Q_{if} = V_i - V_f + W_i - W_f \quad . \tag{4.2}$$

Since we are not interested in the scattering involving transitions between particular rotational states but only in the overall effect of all rotational transitions, we define the effective inelastic energy

transfer $Q_{eff}$ as the average of $Q_{if}$ (defined as follows).

Averaging will be carried out in two steps. In the first step we fix the initial rotational angular momentum J=i and average over all possible final angular momenta J=f by defining

$$Q_i = \sum_f P_{if} Q_{if} \quad , \tag{4.3}$$

where $P_{if}$ are the conditional probabilities for ending in a final state with J=f, given that initially J=i. The possible states are constrained by conservation of energy and total angular momentum. Since at least to our knowledge the quantities $P_{if}$ have not been calculated or measured, we approximate them and then try to argue that the result is not very sensitive to the particular approximation used. In the equal probability approximation we assume that the probabilities for all the possible final states are equal. Then $P_{if}$ is proportional to the degeneracy of the final state, as given by its total angular momentum. More accurate is the neutron approximation, in which we take the probability for ending up in a state with J=f to be the same as for the case of neutron scattering and use the results of Rahman [30]. The degeneracy factor is of course the same as in the equal probability approximation.

In the second and last step we average over the thermal distribution of initial rotational angular momenta

$$Q_{eff} = \sum_i Q_i P_i(T) \quad , \tag{4.4}$$

where $P_i$, the probability for finding the molecule in state i at temperature T, is proportional to the Boltzmann factor and to the

degeneracy of the level due to angular momentum

$$P_i \sim (2I+1)\,(2J+1)\,\exp\left(-\frac{W_i}{kT}\right) \quad . \tag{4.5}$$

Note that 2I+1 equals 1 for even J and 3 for odd J.

To understand the calculations, consider first the case $J_i$=0. Then, by the Pauli principle, I=0. Thus the total angular momentum of the molecule K=0. Suppose the incident atom undergoes a S->T transition. Then the final angular momentum state of the molecule must be K=1 to conserve angular momentum in the collision process. K=1 can come only as J=1, I=1, so in this example the molecule is excited from the J=0 to the J=1 state.

As a second example, consider a S->T transition, where initially the molecular state had J=1, implying I=1, K=2,1,0. Since the muonic atom spin F=0 initially, the total angular momentum $J_T$=K initially. This means the molecule must be left in one of the states K=3,2,1,0, which can come from J=3, I=1; J=2, I=0; J=1, I=1; or J=0, I=0. All other possibilities are excluded by conservation of angular momentum and the Pauli principle.

In this second example our first average (described above) requires knowledge of the branching probabilities to each of the final states characterized by J. We have already noted that $J_T$ equals 0,1 or 2; the probability of these states is 1/9, 1/3 and 5/9, respectively. If $J_T$=0, then after the collision K=1, since F=1. This allows only one possible final state, namely J=1, I=1. The probability of reaching it with $J_T$=0 is 1/9. If $J_T$=1, then K=2,1 or 0 and there are four equally probable final states J=3, I=1; J=2, I=0; J=1, I=1 and J=0, I=0, so the

probability of reaching them through $J_T$=1 is 1/12. For $J_T$=2, K=3,2,1 and the allowed final states are J=3,2,1, all at probability 5/27. Since we only care about the final state and not about the way how it was reached from the given initial state, we sum the probabilities for different $J_T$ yielding the same final state J. This tells us that the molecule goes to the state J=3 with probability 1/12 + 5/27 = 29/108; to the state J=2 with the same probability; to J=1 with probability 1/12 + 5/27 + 1/9 = 41/108 and to J=0 with probability 1/12.

In the neutron approximation, the above probabilities are weighted with the weight of neutron cross sections obtained from Rahman [30], but numerically, there is no significant difference - see Figs.2,3.

The results of the calculation for two different temperatures are presented in Figures 2 to 4. At T=100K, only the lowest two rotational levels were taken into account, since they represent 99% of the ambient population, while at T=300K levels up to J=3 contribute appreciably. Corresponding to the two inelastic processes (T->S and S->T), we have two curves in each figure ($Q_{eff}^{TS}$ and $Q_{eff}^{ST}$, or rather $-Q_{eff}^{ST}$, which is positive and hence more convenient to plot). The curve $|Q|$=.183eV is given for reference since if the rotational transitions are neglected, $Q^{TS}=|Q|$ and $Q^{ST}= -|Q|$. $Q_{eff}$ is a function of the initial kinetic energy of the muonic atom E'. In the equal probability approximation this is due to the fact that at higher E' more final states are allowed by energy conservation, and so $Q_{eff}$ has steps corresponding to the opening of new channels. In addition, in the neutron approximation, the conditional probabilities $P_{if}$ are functions of E'. At least qualitative agreement of the results given by the simple - minded equal probability approximation

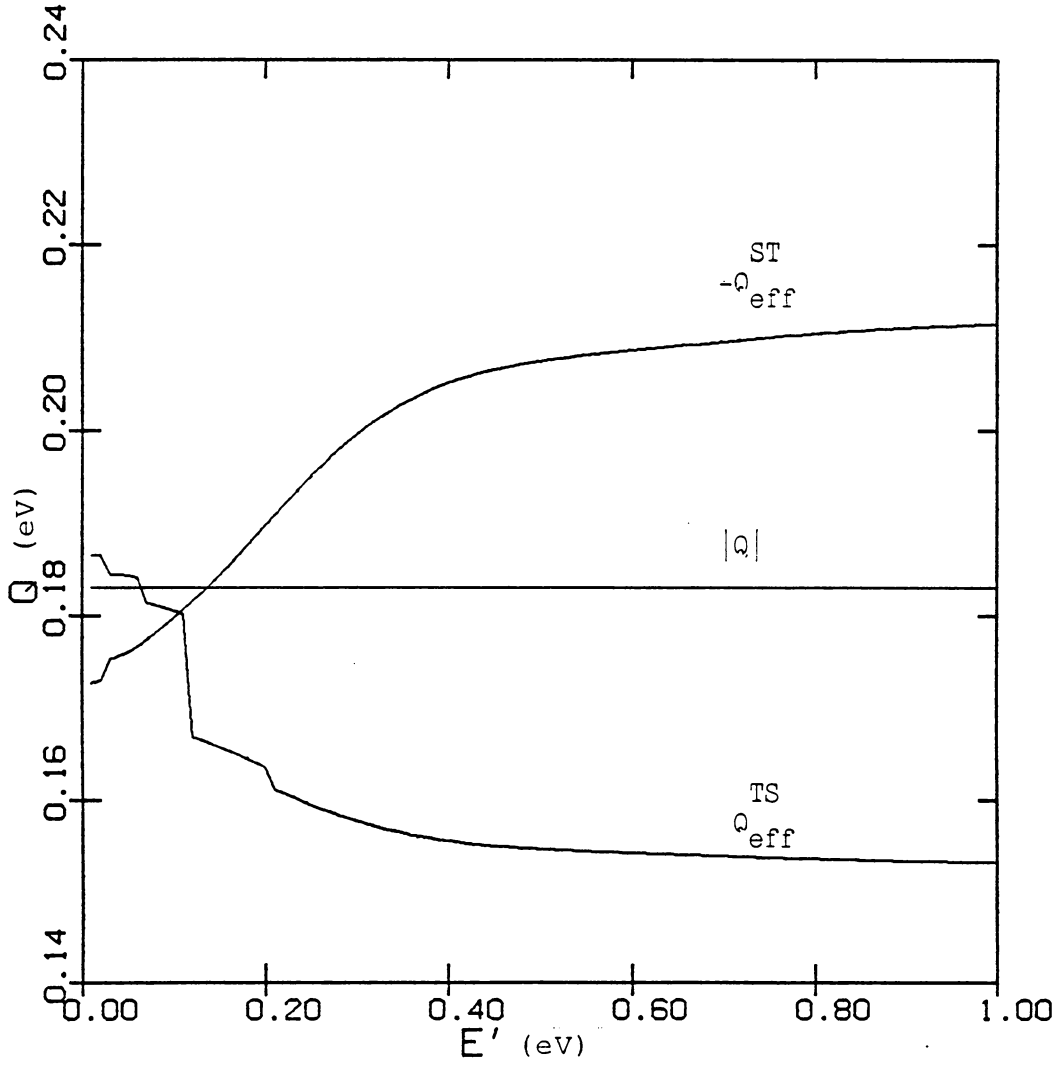


Fig.2 Effective inelastic energy transfers $Q_{eff}^{TS}$ and $-Q_{eff}^{ST}$, as functions of the initial kinetic energy at 300K (neutron approximation).

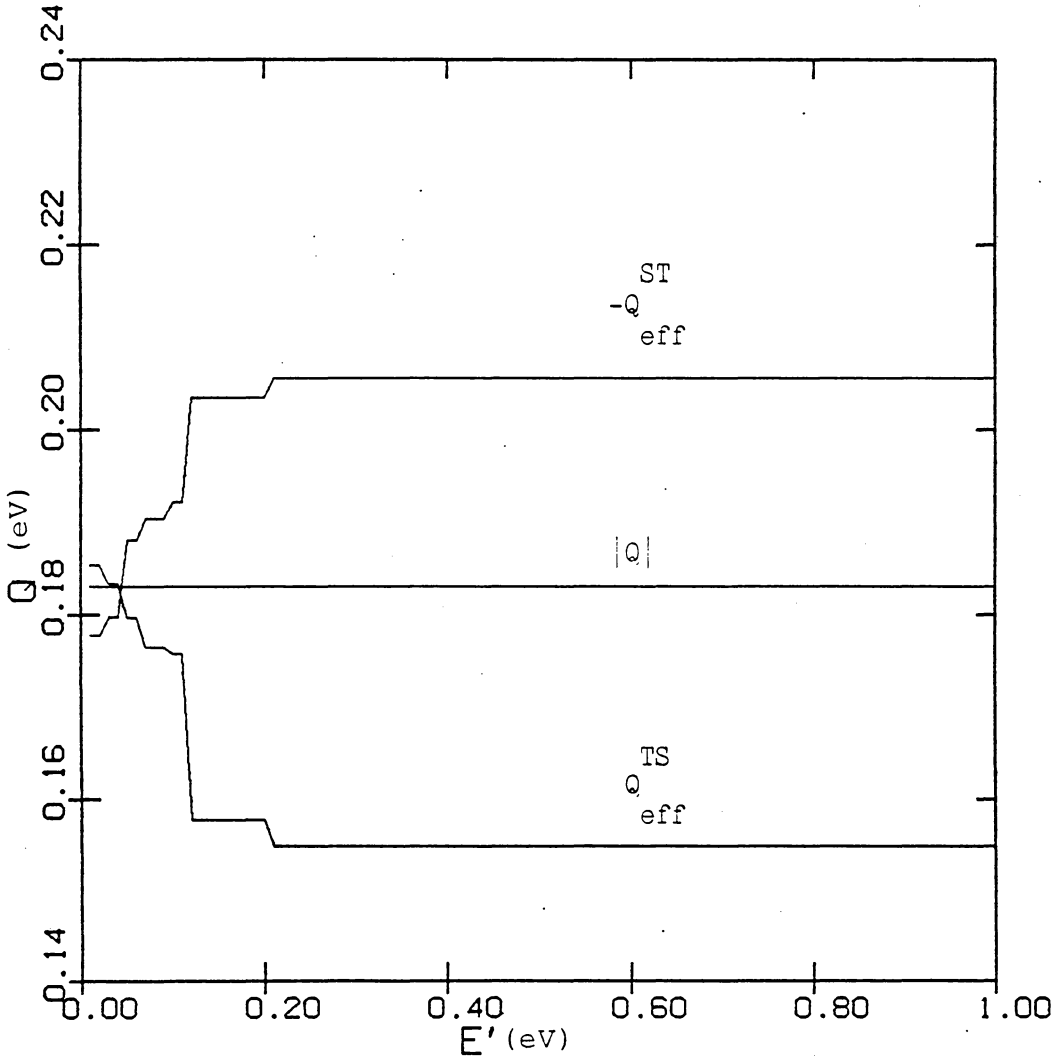


Fig.3 Same as Fig.2, using the equal probability approximation.

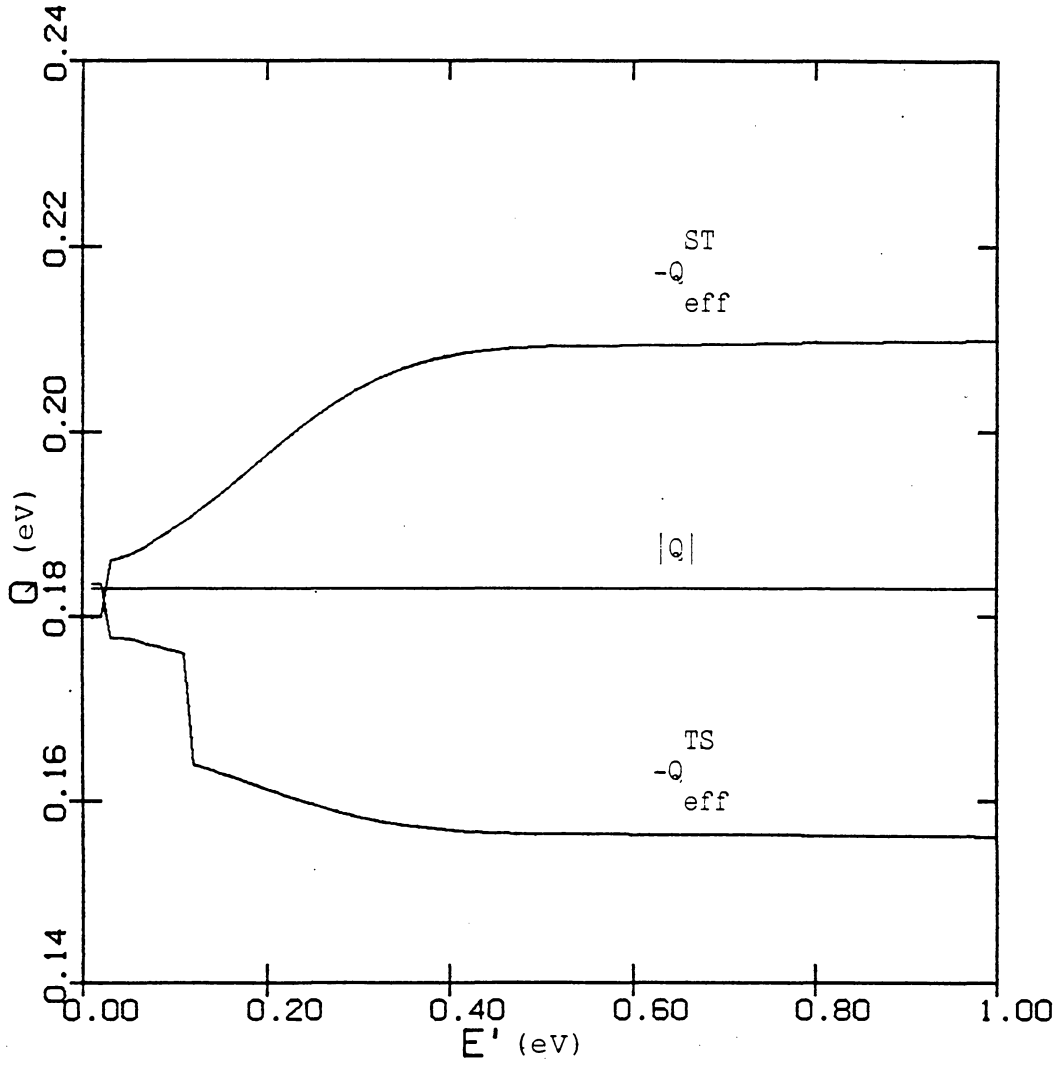


Fig.4 Same as Fig.2, for 100K.

and the neutron approximation shows that the result is not very sensitive to the values of $P_{if}$. Therefore the neutron approximation should give reasonable results.

The results show that the effect of rotations is large enough that it should be taken into account, since $Q_{eff}$ represents a correction of about 15% compared to Q.

## 5. DOPPLER EFFECT

The expressions derived for $\Sigma_0(E'\text{->}E)$ and $\mu_0(E')$ in Sec.3 assume that the target molecules are at rest, i.e. apply strictly only for T=0. For T>0, the thermal motion of the molecule must be considered. The standard procedure [13] is to compute $\Sigma_0$ and $\mu_0$ for a fixed molecule and to average the result over the Maxwellian distribution of these velocities.

The resulting cross section $\Sigma_0(E'\text{->}E;T)$ was first obtained by Wigner and Wilkins [31] for elastic collisions between neutrons and nuclei. This cross section can be used if it is modified in two ways, first for the inelasticity and second for the fact that the scattering centers are bound in molecules. (The available cross section data are for collisions between muonic hydrogen atoms and ordinary hydrogen atoms, not molecules.)

The second correction has been introduced by Messiah [32] for the case of incident neutrons. As we have already explained, the muonic atoms are very similar to neutrons, so the same correction has been adopted. It is

$$\sigma_b = \left( 1.2 + .488 \frac{kT}{E'} \right) \sigma_f \quad , \tag{5.1}$$

where $\sigma_f$ is the "free" cross section, i.e. for unbound hydrogen atoms. The cross section of the hydrogen molecule is then $\sigma_m = 2\sigma_b$. Messiah's theory is based on the assumption that the initial energy of the projectile is large compared to the mean level spacing of the initial rotational states of the target molecule [32]. In effect, this means we can safely apply our theory to muonic atoms whose original energy is

greater than about .01 eV.

The first correction involves introducing $Q_{eff}$ into the Wigner - Wilkins cross section. We begin with the equation (2.18) of Williams [13]:

$$\Sigma(E'->E;\mu_0) = \frac{N\sigma_m}{4\pi}\left(\frac{E}{E'}\right)^{1/2}\frac{1}{2\pi}\int_{-\infty}^{\infty} dt\, \exp\left[-i(E'-E)t - \frac{K^2}{2A}(Tt^2-it)\right] . \tag{5.2}$$

Here N is the number density of hydrogen molecules, T is the temperature and K is the momentum transfer,

$$\frac{1}{2}K^2 = E' + E - 2(E'E)^{1/2}\mu_0 . \tag{5.3}$$

Units in Eqs.(5.2) and (5.3) have been chosen such that $\hbar$=1, k=1 and the muonic atom mass equals 1.

To adapt Eq.(5.2) to inelastic scattering we first multiply the integrand by a factor $\exp(-iQ_{eff}t)$ and secondly, the cross section must be renormalized to have the correct limit as T->0. This requires the replacement

$$\sigma_m \longrightarrow \frac{(A+1)^2}{\beta A^2}\sigma_m . \tag{5.4}$$

The zeroth moment of the cross section is obtained from Eq.(5.2) by integrating over $\mu_0$ and can be written in the form

$$\Sigma_0(E'->E) = \frac{\Sigma(E')(A+1)^2}{8AE'\beta(E')}\left[e^{q+\epsilon'-\epsilon}(\mathrm{erf}(a)-\mathrm{erf}(b)) + \mathrm{erf}(c)-\mathrm{erf}(d)\right] \tag{5.5}$$

with

$$\begin{bmatrix} a \\ c \end{bmatrix} = \frac{1}{2A^{\frac{1}{2}}} \left( \epsilon'^{\frac{1}{2}} + \epsilon^{\frac{1}{2}} \right) \begin{bmatrix} + \\ - \end{bmatrix} \frac{A^{\frac{1}{2}}}{2} \frac{q + \epsilon' - \epsilon}{(\epsilon'^{\frac{1}{2}} + \epsilon^{\frac{1}{2}})} \tag{5.6}$$

$$\begin{bmatrix} b \\ d \end{bmatrix} = \frac{1}{2A^{\frac{1}{2}}} \left| \epsilon'^{\frac{1}{2}} - \epsilon^{\frac{1}{2}} \right| \begin{bmatrix} + \\ - \end{bmatrix} \frac{A^{\frac{1}{2}}}{2} \frac{q + \epsilon' - \epsilon}{\left| \epsilon'^{\frac{1}{2}} - \epsilon^{\frac{1}{2}} \right|} ,$$

where

$$q = \frac{Q}{T} , \qquad \epsilon' = \frac{E'}{T} , \quad \epsilon = \frac{E}{T} . \tag{5.7}$$

To help appreciate the importance of the Doppler correction we show in Fig.5 $\Sigma_0(E' \rightarrow E)$ as a function of E, for E'=1eV, at 300K and at 0K. In Fig.6 we show $\mu_0(E')$ versus E' for the same two temperatures.

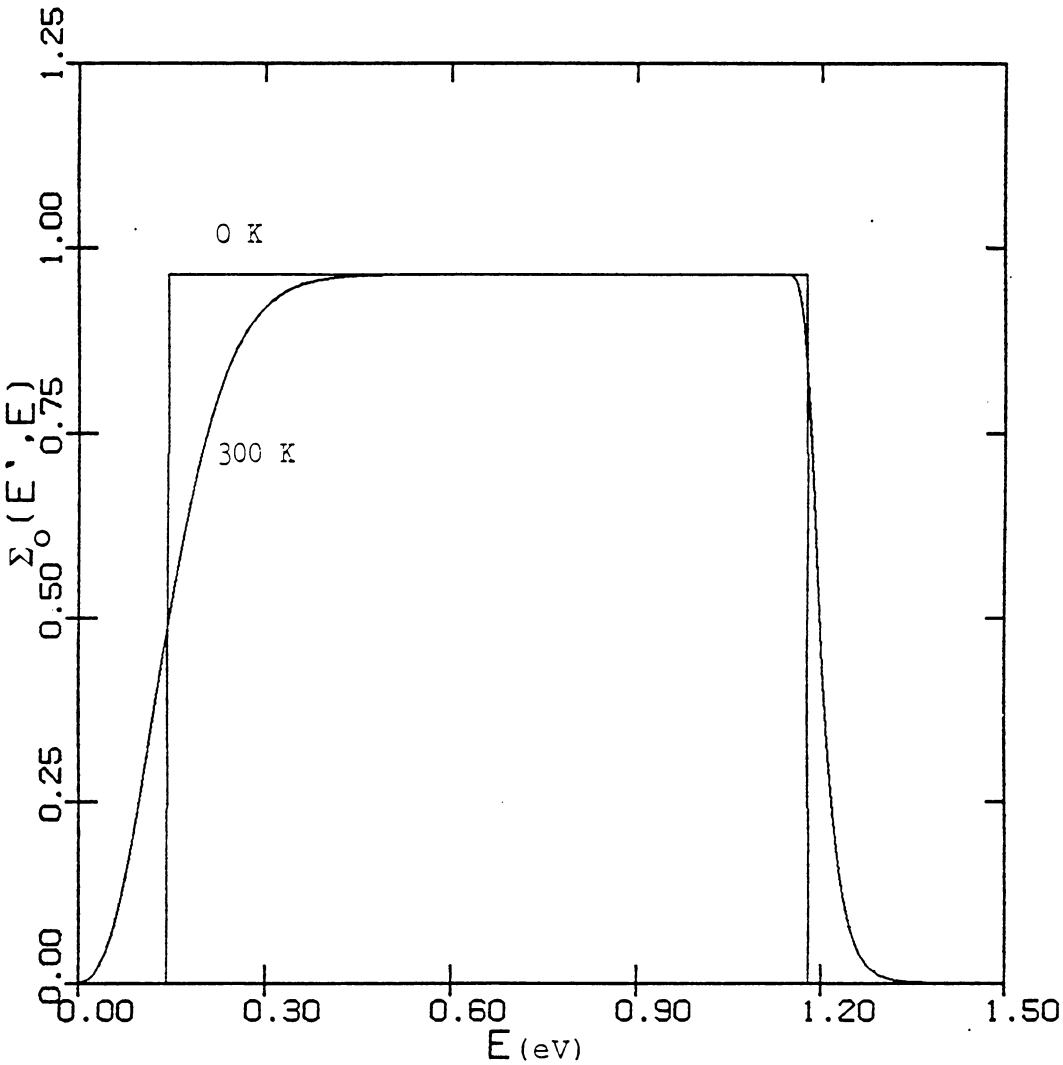


Fig.5 The zeroth moment of the scattering cross section $\Sigma_0(E'->E)$, as a function of E, for E'=1eV, at 300K and at 0K.

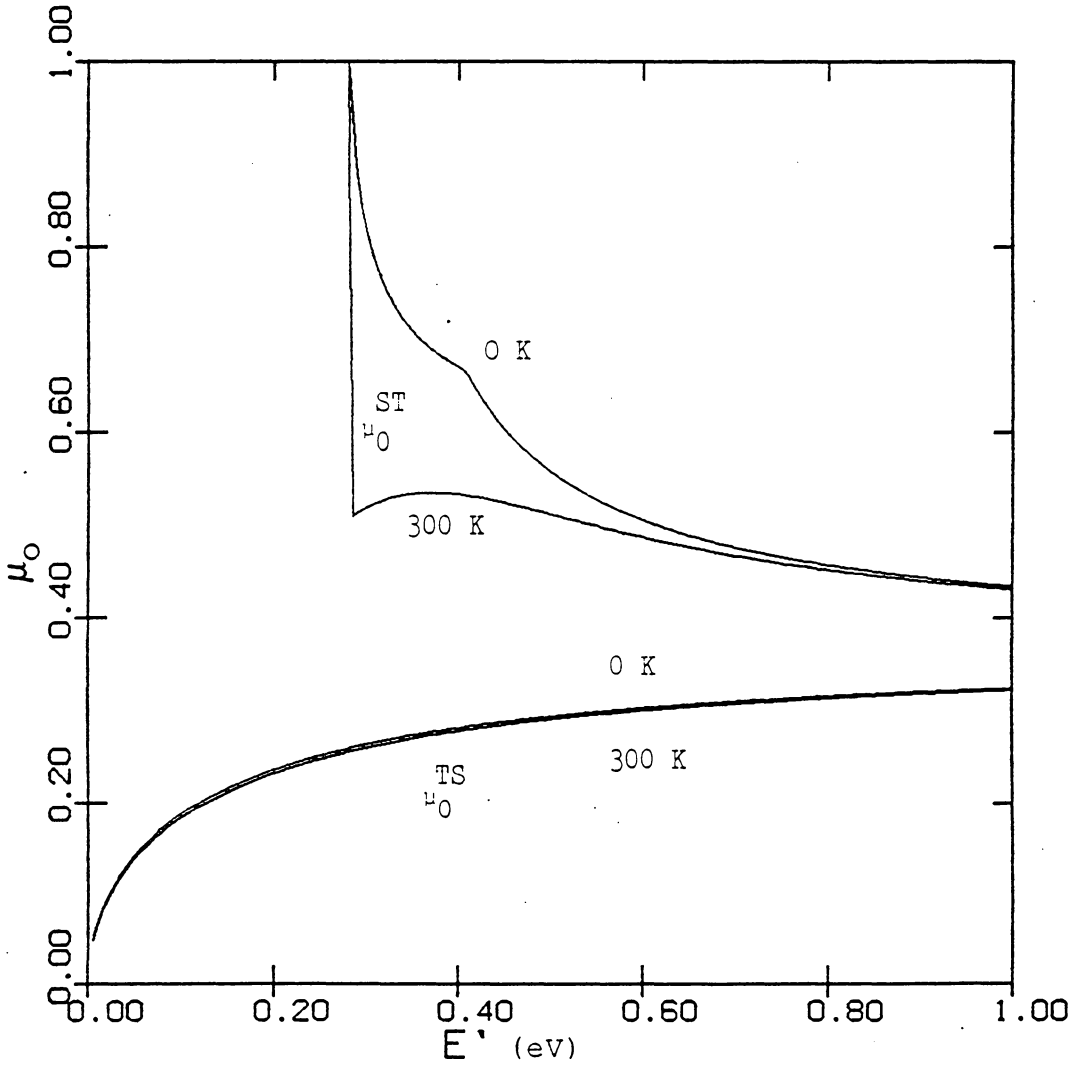


Fig.6 The average cosines of the scattering angle $\mu_0^{ST}(E')$ and $\mu_0^{TS}(E')$, at 300K and at 0K.

## 6. THE UNCOLLIDED FLUX

The accuracy of the diffusion approximation can be improved considerably by separating the uncollided flux $\Phi^u$ and using the first collisions as the source for the diffusion equation. Clearly, $\Phi^u$ can be defined analytically, as follows.

The initial source of muonic atoms is isotropic and independent of x, so $\Phi^u$ satisfies

$$\frac{1}{v_0}\frac{\partial\Phi^u(t,x,\mu)}{\partial t} + \mu\frac{\partial\Phi^u}{\partial x} + \Sigma(E_0)\Phi^u = S_0\,\delta(t)\,\delta(E-E_0) \quad , \tag{6.1}$$

where $S_0$ is the source strength (atoms/cm). The Laplace transform of Eq.(6.1) gives

$$\frac{p}{v_0}\hat{\Phi}^u(p,x,\mu) + \mu\frac{\partial\hat{\Phi}^u}{\partial x} + \Sigma\hat{\Phi}^u = S_0\,\delta(E-E_0) \quad . \tag{6.2}$$

Here p is the transform variable and $\hat{\Phi}^u(p,x,\mu)$ the transformed flux. Since we are only interested in the solution inside the slab ($|x| < d/2$), we may consider $\Sigma$ and $S_0$ as constants, independent of x. The equations for singlet and triplet are decoupled, so it suffices to solve for one species:

$$\hat{\phi}^u_a(p,x,\mu) = \frac{S_0 v_0}{p + \Sigma_a v_0}\left[1 - \exp\left[-\frac{p + \Sigma_a v_0}{\mu\, v_0}\left(x + \frac{d}{2}\right)\right]\right] \tag{6.3a}$$

$$|x| < d/2,\ \mu > 0,\ a = S,\ T$$

and

$$\hat{\phi}^u_a(p,x,\mu) = \frac{S_0 v_0}{p + \Sigma_a v_0}\left[1 - \exp\left[\frac{p + \Sigma_a v_0}{\mu\, v_0}\left(\frac{d}{2} - x\right)\right]\right] . \tag{6.3b}$$

$$|x| < d/2,\ \mu < 0,\ a = S,\ T$$

Performing the Laplace inversion yields

$$\phi_a^u(t,x,\mu) = S_0 v_0 \exp(-\Sigma_a v_0 t) \begin{cases} 1 - H(\mu v_0 t - x - \frac{d}{2}) & \text{if } \mu>0 \\ 1 - H(\mu v_0 t - x + \frac{d}{2}) & \text{if } \mu<0 \end{cases}, \tag{6.4}$$

where H(x) is the Heavyside function

$$H(q) = \begin{cases} 1, & q > 0 \\ 0, & q < 0 \end{cases} . \tag{6.5}$$

As we shall see, we need only the zeroth moment $\phi^u_{0a}$ (as a source for the collided flux) and the first moment $\phi^u_{1a}$ (to obtain the emergent flux). They can be computed by integration, recalling Eq.(6).

$$\phi^u_{0a}(t,x) = S_0 v_0 \exp(-\Sigma_a(E_0)v_0 t) \left[ 2 - (1 - \frac{d/2 - x}{v_0 t}) H(v_0 t - \frac{d}{2} + x) \right.$$
$$\left. - (1 - \frac{x + d/2}{v_0 t}) H(v_0 t - x - \frac{d}{2}) \right] \tag{6.6a}$$

and

$$\phi^u_{1a}(t,x) = \frac{S_0 v_0}{2} \exp(-\Sigma_a(E_0)v_0 t) \left[ \left[1 - \left[\frac{d/2 - x}{v_0 t}\right]^2\right] H(v_0 t - \frac{d}{2} + x) \right.$$
$$\left. - \left[1 - \left[\frac{x + d/2}{v_0 t}\right]^2\right] H(v_0 t - x - \frac{d}{2}) \right] . \tag{6.6b}$$

The quantity that is usually measured in an experiment is the emerging flux X(t), i.e. the number of atoms escaping from the slab per second. As in the case of the flux, we can write it as a sum of the uncollided part $X^u$ and the collided part $X^c$, where

$$X_a^u(t) = 2\,\phi_{1a}^u(t,d/2) =$$

$$= S_0 v_0 \exp(-\Sigma_a(E_0)v_0 t) \begin{cases} 1 & , \quad v_0 t < d \\ \left[\frac{d}{v_0 t}\right]^2 & , \quad v_0 t > d \end{cases} \quad . \tag{6.7}$$

Integration over all times and setting $S_0 = (2d)^{-1}$ (corresponding to a single atom inside the slab at t=0), yields the ratio of atoms that eventually escape from the slab without suffering a single collision (escape probability [3])

$$U(\delta_a) = \frac{1}{2}\left[\frac{1}{\delta_a}\left(1 - e^{-\delta_a}\right) + E_2(\delta_a)\right] \quad , \tag{6.8}$$

where $\delta_a = \Sigma_a d$ is the optical width for the atoms in state a and $E_2(x)$ is the exponential integral

$$E_2(x) = \int_1^\infty e^{-xt}\, t^{-2}\, dt \quad . \tag{6.9}$$

This quantity can give insight into the applicability of the diffusion approximation and/or multiple collision expansion.

We will also need the $n^{th}$ Fourier component of the total uncollided flux

$$\phi_{0na}^u(t) = \frac{8\, S_0\, d}{(2n-1)^2\pi^2} \exp(-v_0\Sigma_a(E_0)t) \quad x$$

$$\left[1 + \frac{\sin(2n-1)\pi\tau}{(2n-1)\pi\tau} - \left[1 - \frac{1}{\tau} + \frac{\sin(2n-1)\pi\tau}{(2n-1)\pi\tau}\right] H(\tau-1)\right] \quad , \tag{6.10}$$

where

$$\tau = \frac{v_0 t}{d} \quad . \tag{6.11}$$

## 7. NUMERICS

As we mentioned in the previous section, the accuracy of the diffusion approximation can be improved by separating the uncollided flux. The $n^{th}$ Fourier component of the collided flux $\Phi^c_{0n}(t,E)$ then obeys the zero initial condition and satisfies Eq.(2.17) with the right hand side supplemented by the source:

$$S_n(t) = \begin{bmatrix} \Sigma_{SS}(E_0) & \Sigma_{TS}(E_0) \\ \Sigma_{ST}(E_0) & \Sigma_{TT}(E_0) \end{bmatrix} \Phi^u_{0n}(t) \quad , \tag{7.1}$$

where $\Phi^u_{0n}$ was defined by Eq.(6.10).

We solve the resulting equation:

$$\frac{1}{v}\frac{\partial\Phi^u_{0n}(t,E)}{\partial t} + (D(E)B_n^2 + \Sigma(E))\,\Phi^u_{0n} = \int \Sigma_0(E'\to E)\,\Phi^u_{0n}(t,x,E')\,dE' + S_n(t) \tag{7.2}$$

numerically, using the following scheme. As is usually done in neutron transport, we discretize the energy variable by the multigroup method. First, we define K energy intervals $I_k = [E_{k-1},E_k]$, k=1,...,K. Assuming that the flux in each group is independent of energy, i.e. it is constant on $I_k$, we can write:

$$\Phi_{0n}(t,E) = \sum_{k=1}^{K} \Phi_k(t)\,\chi_{I_k} \quad , \tag{7.3}$$

where $\chi_{Ik}$ denotes the characteristic function of the k-th interval and the indices 0, n and u on $\Phi_k$ have been suppressed for the sake of clarity. Using the ansatz (7.3) in Eq.(7.2) and integrating over $I_k$ yield:

$$\frac{d\Phi_k(t)}{dt} = \left[\frac{2}{m}\right]^{\frac{1}{2}} (E_k^{\frac{1}{2}} - E_k^{\frac{1}{2}}) \left[ - (D_k B_n^2 + \Sigma_k)\, \Phi_k(t) + \sum_i \Sigma_{ki}\, \Phi_i(t) + S_k(t)\right] , \tag{7.4}$$

with

$$D_k = \int_{I_k} D(E)\, dE \quad , \tag{7.5a}$$

$$\Sigma_k = \int_{I_k} \Sigma(E)\, dE \quad , \tag{7.5b}$$

$$\Sigma_{ki} = \int_{I_k} dE \int_{I_i} \Sigma(E'->E)\, dE' \quad , \tag{7.5c}$$

and m is, of course, the mass of the muonic atom. Now, Eq.(7.4) is just a system of ordinary differential equations for $\Phi_k$ and can be written in vector form:

$$\frac{d\Phi(t)}{dt} = A\, \Phi(t) + b(t) \quad . \tag{7.6}$$

By approximating the time derivative by the forward difference, we obtain an explicit numerical scheme:

$$\Phi(t+\Delta t) = \Phi(t) + [A\, \Phi(t) + b(t)]\, \Delta t \quad , \tag{7.7}$$

where the knowledge of $\Phi(t)$ suffices for the calculation of $\Phi(t+\Delta t)$. As usually with explicit numerical schemes, care must be taken when choosing the timestep $\Delta t$, in order to insure numerical stability [33,34]. This restricts $\Delta t$ to be less or equal to about one tenth of the mean collision time, but the payoff, compared to an implicit scheme, is that no matrix inversion is required.

## 8. RESULTS

Using the numerical scheme, described in the previous section and implemented in the code DIFF.FOR (See Appendix), we solve the diffusion equation for a number of initial data. The first three terms in the Fourier expansion were retained and twenty energy groups were used with time step $\Delta t$ = 1ns.

We present the results of several calculations for the case of deuterium (Fig.7-9) and hydrogen (Fig.10). The atomic cross sections (Ref.35 for hydrogen and Ref.36 for deuterium) were used and converted to molecular cross sections, as explained in Sec.5. Since the above references only provide three of the four cross sections, namely $\sigma_{SS}$, $\sigma_{ST}$ and $\sigma_{TT}$, we used reciprocity to obtain the fourth one:

$$\sigma_{TS}(E) = \frac{1}{3} \frac{E + Q}{E} \sigma_{ST}(E) \quad , \tag{8.1}$$

where, in the case of hydrogen, Q=0.183. For deuterium, the spin factor 1/3 must be replaced by 1/2 (doublet and quartet states) and Q=0.049. In the case of hydrogen, the effect of rotations of the scatterers was taken into account by replacing the hyperfine splitting constant (Q=.183eV) with the effective inelastic energy transfer, $Q_{eff}(E)$, as defined in Sec.4. For deuterium, however, the hyperfine splitting is small (Q=.049), so this correction was ignored. Only the emerging flux $X(t) = X_S + X_T$ is plotted, since present experiments cannot distinguish between the atoms in the two hyperfine states.

Fig.7 shows the effect of varying the initial energy $E_0$ ($E_0$=1eV, 0.5eV, 0.1eV) in the case of deuterium diffusing in a slab of width d=1cm, at p=1bar and T=300K. Diffusion at two different temperatures

T=300K and T=200K is shown on Fig.8, for d=1cm, p=1bar, $E_0$=1eV. Finally, pressure has been varied on Fig.9, for d=1cm, T=300K, $E_0$=1eV.

Diffusion in hydrogen is more interesting because the cross sections vary as a function of energy over two orders of magnitude. The initial statistical mixture (75% triplet, 25% singlet) changes into predominantly singlet during the first few average collision times. Atoms in the singlet state have smaller cross section and hence diffuse faster. This results in a bump on the emerging flux curve (the case d=5cm, p=1bar, T=300K, $E_0$=1eV is shown on Fig.10). The prediction of the bump, though surprising when it was first obtained, was confirmed by a very simple model, which is presented in the following section.

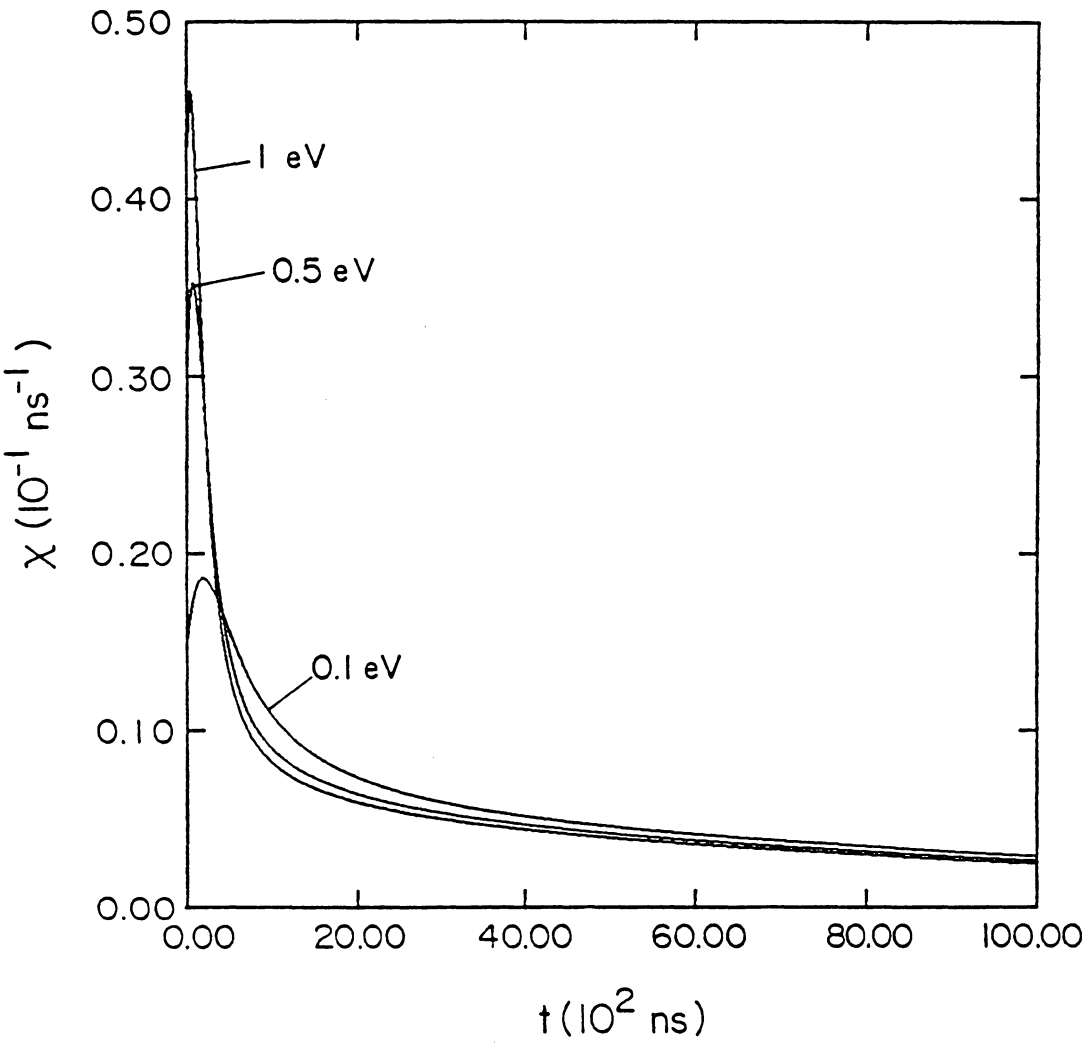


Fig.7 Emerging flux for deuterium diffusing in a slab of width d=1cm, at p=1bar and T=300K, varying $E_0$.

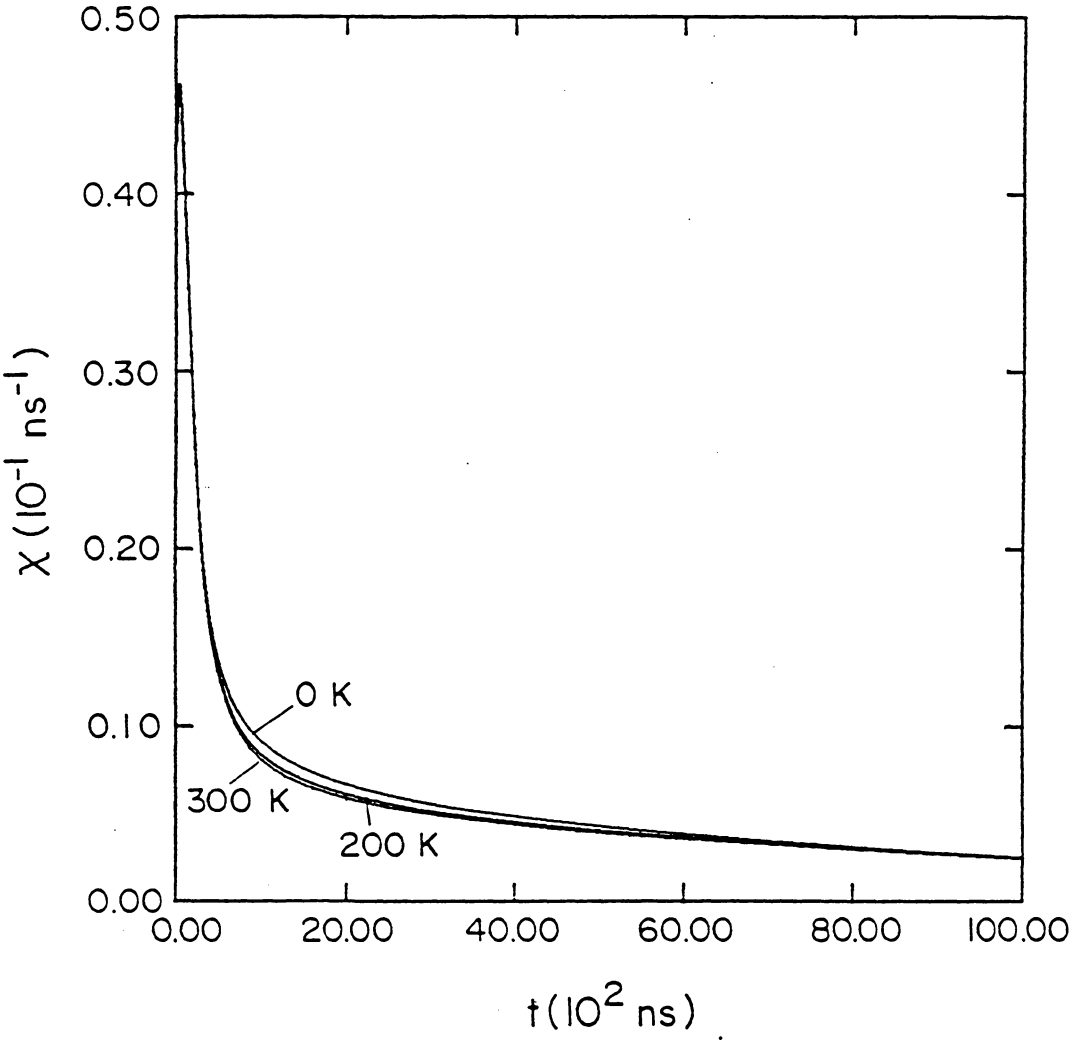


Fig.8 Same as Fig.7, for d=1cm, p=1bar, $E_0$=1eV, varying T.

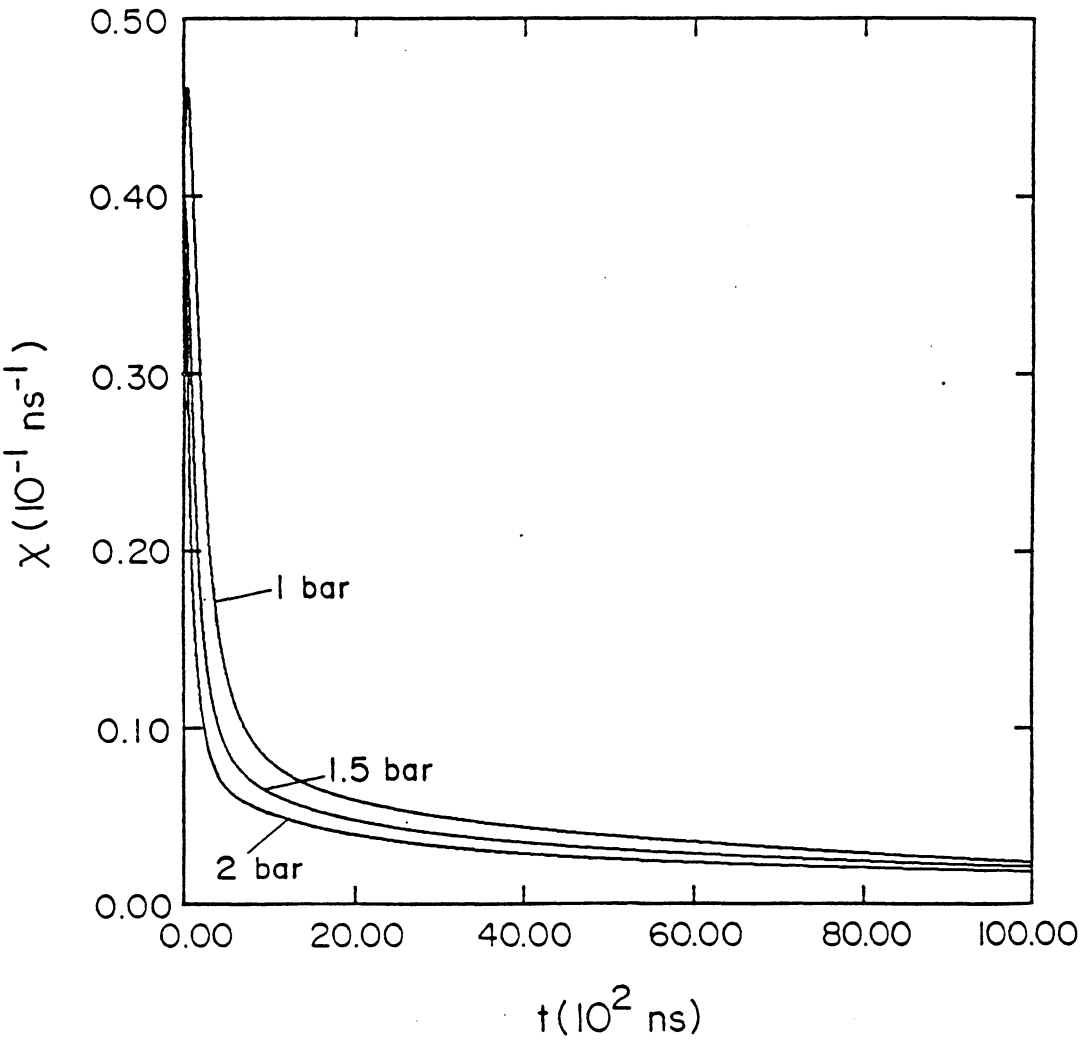


Fig.9 Same as Fig.7, for d=1cm, T=300K, $E_0$=1eV, varying p.

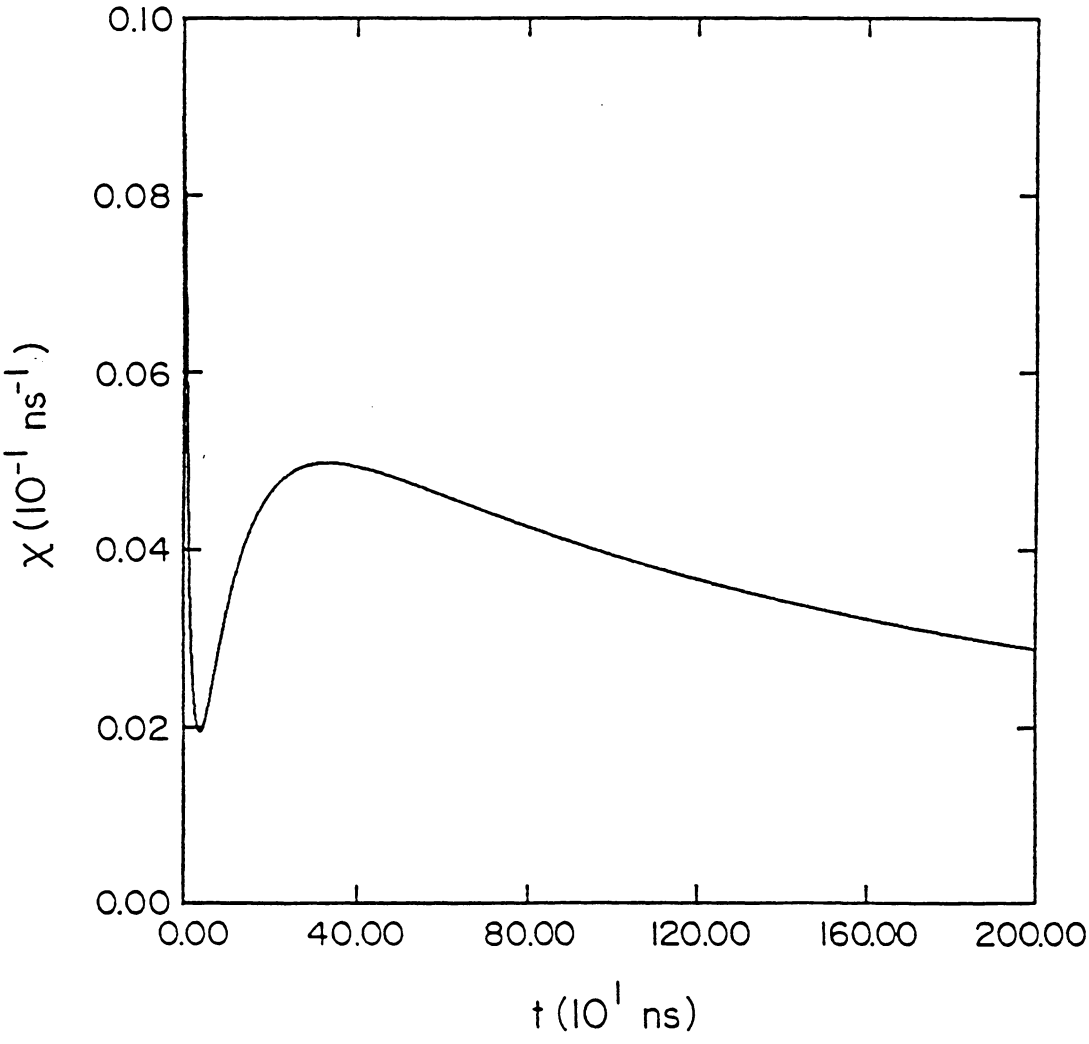


Fig.10 Emerging flux for hydrogen diffusing in a slab of width d=5cm, p=1bar, T=300K, $E_0$=1eV.

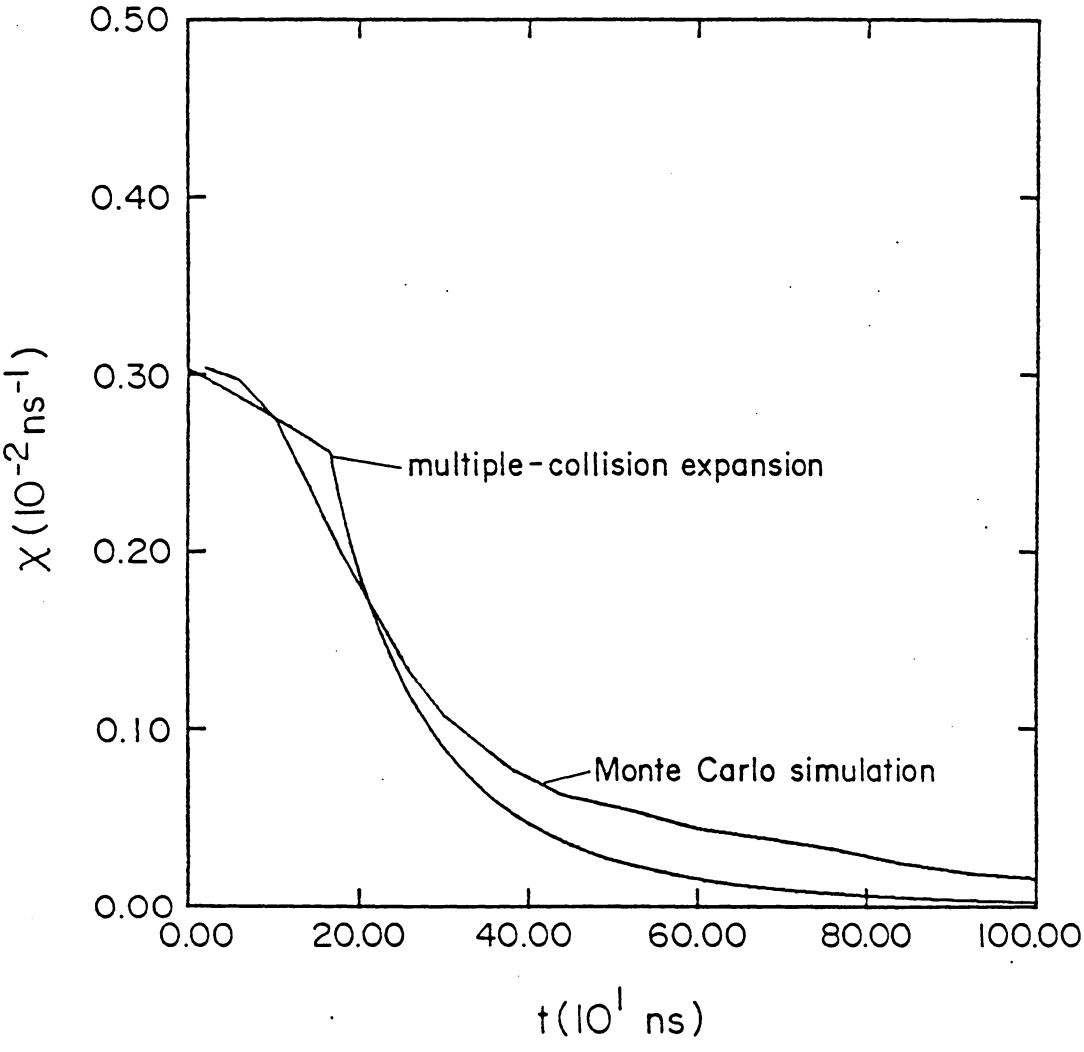


Fig.11 Comparison of the multiple collision expansion with the Monte Carlo simulation for deuterium, d=0.23cm, p=0.188bar, T=300K, $E_0$=2eV.

## 9. ONE-SPEED MODEL

Here we present the analytically solvable one speed model, in which all the atoms are assumed to be moving with the same speed v. Simple as it is, the model reasonably describes the diffusion process, in particular it predicts the bump on the emerging flux curve in the case of hydrogen.

Under the one speed assumption and neglecting the off-diagonal elements in the diffusion matrix D, the diffusion equation (13) yields

$$\frac{\partial \Phi_{0n}(t)}{\partial t} = v \begin{bmatrix} -\Sigma_{ST} - B_n^2 D_{SS} & \Sigma_{TS} \\ \Sigma_{ST} & -\Sigma_{TS} - B_n^2 D_{TT} \end{bmatrix} \Phi_{0n}(t) , \tag{9.1}$$

where the matrix is constant. The main contribution comes from the first Fourier mode, so we set n=1. To simplify the notation we rewrite Eq.(9.1) as

$$\frac{\partial \Psi(t)}{\partial t} = \begin{bmatrix} -\sigma_S - \lambda_S & \sigma_T \\ \sigma_S & -\sigma_T - \lambda_T \end{bmatrix} \Psi(t) . \tag{9.2}$$

In the case of hydrogen, the initial condition is

$$\Psi(t=0) = \frac{1}{4} \begin{bmatrix} 1 \\ 3 \end{bmatrix} . \tag{9.3}$$

The eigenvalues and eigenvectors are

$$\omega_{\pm} = \frac{1}{2}\left[ - \lambda_S - \lambda_T - \sigma_S - \sigma_T \pm \left( (\lambda_S-\lambda_T+\sigma_S-\sigma_T)^2 + 4\sigma_S\sigma_T \right)^{\frac{1}{2}} \right] \tag{9.4a}$$

and

$$v_{\pm} = \begin{bmatrix} 1 \\ u_{\pm} \end{bmatrix} , \qquad u_{\pm} = \frac{1}{\sigma_T} \left( \omega_{\pm} + \lambda_S + \sigma_S \right) \tag{9.4b}$$

and the solution of Eq.(9.3) is a sum of two exponentials

$$\Psi(t) = C_+ v_+ \exp(\omega_+ t) + C_- v_- \exp(\omega_- t) , \tag{9.5a}$$

with

$$C_+ = \frac{3 - u_-}{4 (u_+ - u_-)} , \qquad C_- = \frac{1}{4} - C_+ . \tag{9.5b}$$

In the thermal region $\sigma_S=0$ and the solution (9.5) simplifies into

$$\Psi(t) = \begin{bmatrix} \left[ \frac{1}{4} - \frac{3\,\sigma_T}{4(\lambda_S-\lambda_T-\sigma_T)} \right] e^{-\lambda_S t} + \frac{3\,\sigma_T}{4(\lambda_S-\lambda_T-\sigma_T)} \; e^{-(\lambda_T+\sigma_T)t} \\ \frac{3}{4} \; e^{-(\lambda_T+\sigma_T)t} \end{bmatrix} . \tag{9.6}$$

We are interested in seeing when the emerging flux,

$$X = \lambda_S \psi_S + \lambda_T \psi_T , \tag{9.7}$$

exhibits a bump. Since $\lambda_T$ is much smaller than $\lambda_S$, we ignore it. Then X has a maximum at

$$t = \frac{1}{\sigma_T - \lambda_S} \ln \frac{3\,\sigma_T^2}{\lambda_S(4\sigma_T-\lambda_S)} , \tag{9.8}$$

subject to the condition

$$3\,\sigma_T > \lambda_S \quad , \tag{9.9}$$

which is the requirement of optically thick slab, needed for the validity of the diffusion approximation in the first place.

The one speed model of course cannot predict the initial decay in the emerging flux, which is due to slowing down.

## 10. MULTIPLE SCATTERING EXPANSION

In optically thin media, the diffusion approximation is not valid. Most atoms escape from the medium without suffering a single collision. In this case it is convenient to use the multiple collision expansion for the angular flux $\Phi$ [26,27]

$$\Phi = \Phi^u + \sum_{n=1}^{\infty} \Phi^{(n)} \quad , \tag{10.1}$$

where $\Phi^{(n)}$ is the n times collided flux.

Here we present a low order implementation of Eq.(10.1), in which we retain only $\Phi^u$ and $\Phi^{(1)}$, and neglect the rest. $\Phi^u$ is defined analytically by Eq.(17). Clearly, the source for $\Phi^{(1)}$ are first collisions. We take this source to be isotropic, which is a good approximation. Furthermore, we assume that all atoms contributing to $\Phi^{(1)}$ travel with the average speed $v_1$, i.e. we model the continuous speed distribution of $\Phi^{(1)}$ by $\delta(v-v_1)$. In the case of elastic scattering,

$$v_1 = \frac{3\,A^2 + 1}{3\,A\,(A+1)}\, v_0 \quad , \tag{10.2}$$

where A is the ratio of the masses of the target molecule and the muonic atom.

Then $\Phi^{(1)}$ obeys the equation

$$\frac{1}{v_1}\frac{\partial \Phi^{(1)}(t,x,\mu)}{\partial t} + \mu \frac{\partial \Phi^{(1)}}{\partial x} + \Sigma(E_1)\Phi^{(1)} = S^{(1)}(t,x) \quad , \tag{10.3}$$

where $E_1=mv_1^2/2$ and the source $S^{(1)}$ equals

$$S^{(1)}(t,x) = \frac{1}{2}\begin{bmatrix} \Sigma_{SS}(E_0) & \Sigma_{TS}(E_0) \\ \Sigma_{ST}(E_0) & \Sigma_{TT}(E_0) \end{bmatrix} \Phi_0^u(t,x) \quad , \tag{10.4}$$

Eq.(10.3) can be readily solved by integration along the characteristics [3] and yields:

$$\phi_a^{(1)}(t,x,\mu) = \int_0^t \exp(-\Sigma_a(E_1)v_1(t-\tau))\ S_a(\tau,x-\mu v_1(t-\tau))\ d\tau \ . \tag{10.5}$$

The once collided emerging flux $X^{(1)}(t)$,

$$X^{(1)}(t) = 2\int_0^1 \mu\ \Phi^{(1)}(t,d/2,\mu)\ d\mu \quad , \tag{10.6}$$

can be found by numerical quadrature. The trapezoidal rule was used for numerical evaluation of formulas (10.5) and (10.6).

We employed the above calculation in the case of deuterium muonic atoms in a slab of width d=0.23cm, filled with gaseous deuterium at pressure p=0.188bar and T=300K, which corresponds to optical thickness $\delta$=.52. These parameters were used in an experiment done by R. Siegel [25]. From Eq.(21) we see that 55% of the atoms contribute to the uncollided emerging flux, while numerical integration shows that 26% contribute to the first collided emerging flux. Thus we are ignoring 19% of the atoms, namely those that suffer more than one collision on their way out of the slab.

Unfortunately, the analysis of the experiment has not been completed yet, so we can only compare our calculation with a Monte Carlo simulation

[25]. Although the agreement is apparently good, the two should not be compared directly, because in the experiment the source of muonic atoms is not a delta function in energy, but rather a continuous distribution. In the Monte Carlo simulation this distribution is taken to be a Maxwellian. The calculation gives the Green's function of the problem, while the experiment yields its convolution with the initial source. We hope that comparison of our calculation with the experiment will yield some information about the energy distribution of the source. We plan to improve the calculation by taking into account more terms in the multiple collision expansion.

## 11. CONCLUSION

This work is opening a new area of transport theory - transport of muonic atoms. As we have seen, this transport is in many respects similar to neutron transport so that many techniques from neutron transport theory can be used or generalized.

However, there are also several interesting new features. First, transport of muonic atoms is a transport of two interacting species (generalization to n is straightforward). Second, collisions that involve conversions from one species to another are inelastic. Consequently, the scattering cross sections have a more complicated energy dependence and they involve the inelasticity parameter Q. Finally, the evolution of a system with more than one species is richer, compared to the one-species case. For example, the emerging flux need not be a monotonically decreasing function of time.

The time-dependent problem that we considered received relatively little attention in neutron transport [37,41], because reactor calculations are primarily concerned with the stationary state.

At the end we would like to mention some possibilities for future work. We treated the optically thick slab by the diffusion approximation and the optically thin slab by the multiple collision expansion. The latter was only carried out to low order and it seems a worthwhile project to develop it more fully. Also, the intermediate case cannot be covered by either of them, so a direct numerical solution of the transport equation (2.3) by the, say, $S_N$ method is suggested. Finally, problems motivated by the muon catalyzed fusion, involving more than one hydrogen isotope, offer a whole new area of research.

## APPENDIX

Numerical calculations represent an important part of this work and here we present the codes that we used (and wrote). The programs are easy to use and entering input from the terminal, when necessary, is self-explanatory.

Program THICK solves the diffusion equation, as described in Sec.7 both for the case of hydrogen and deuterium. As input, it needs the cross sections (file 21 for hydrogen, file 22 for deuterium), the average of the scattering angle (file 12) and, in the case of hydrogen, the effective inelastic energy transfer $Q_{eff}$ (file 11). Various parameters that the program needs, such as the timestep $\Delta t$, the number of Fourier modes considered and the number of iterations, are given in file 7. The results, namely X(t), appear in file 8.

The multiple collision expansion, appropriate for optically thin slabs, is implemented in program THIN. No input files are needed and the output X(t) is given in file 1.

Finally, program Q calculates the effective inelastic energy transfer $Q_{eff}$. Again, no input is needed and file 11 contains the results.

```
C
C                 program THICK
C
      IMPLICIT REAL*8(A-H,O-Z)
C
      DIMENSION E(20), EPL(20), EPH(20), EML(20), EMH(20), SIGT(20)
      DIMENSION SIGSS(20), SIGST(20), SIGS(20), SIGTS(20), SIGTT(20)
      DIMENSION PSS(20,20), PST(20,20), PTS(20,20), PTT(20,20)
      DIMENSION FIS(2,22), FIT(2,22), PSIS(22), PSIT(22)
      DIMENSION FIS0(2,22), FIT0(2,22), PSIS0(22), PSIT0(22)
      DIMENSION DIFST(22), DIFTS(22), DIFSS(22), DIFTT(22)
      DIMENSION I1(20)
      DIMENSION B(20)
      DIMENSION SLEFT(1000), TLEFT(1000)
      DIMENSION OUT(1000), OUTS(1000), OUTT(1000)
      DIMENSION ratioel(20), ratiost(20), ratiots(20)
C     COMMON /A/SIGSS, SIGST, SIGS, SIGTS, SIGTT, SIGT
      COMMON /INI/ ANGST(22), ANGTS(22), QST(22), QTS(22)
      COMMON /SMALL/ A, T
      DATA OUT/1000*0.0/
      DATA OUTS/1000*0.0/
      DATA OUTT/1000*0.0/
      DATA SLEFT/1000*0.0/
      DATA TLEFT/1000*0.0/
    1 FORMAT(2x,f10.2,6(2X,F11.6))
    3 FORMAT(4(2X,F12.8))
    2 FORMAT(20I5)
    4 FORMAT(7(2X,I9))
      write(*,*) ' PLEASE CHOOSE:  1 = hydrogen, 2 = deuterium)'
      read(*,*) ihd
      IF (ihd.eq.1) fac1 = 25.
      IF (ihd.eq.1) fac2 = 75.
      IF (ihd.eq.2) fac1 = 100. / 3.
      IF (ihd.eq.2) fac2 = 200. / 3.
      READ(7,*) NN
      READ(7,*) DT
      READ(7,*) NFMAX
      READ(7,*) ENOUGH
      READ(7,*) KMAX
      WRITE(*,*) ' TIME STEP = ', real(DT)
      WRITE(*,*) ' NO. OF FOURIER MODES = ', NFMAX
c     WRITE(*,*) ' ENOUGH = ENOUGH = ', ENOUGH
      WRITE(*,*) ' MAXIMAL NO. OF ITERATIONS = ', KMAX
      ns = 10
      nplot = 1
c     IF (kmax.gt.500) nplot = (kmax+1)/500
300   CONTINUE
      write(*,*) ' D = ? cm     (total slab width)'
      write(*,*) '              (single spacing = .23cm)'
      read(*,*) d
c     d = d * 2.54
      IF (d.lt.0) GO TO 120
      write(*,*) ' E0 = ? eV'
      read(*,*) E0
      IF (E0.lt.0) GO TO 120
      write(*,*) ' p = ? bar'
      read(*,*) press
      IF (press.lt.0) GO TO 120
      write(*,*) ' T = ? K'
      read(*,*) t
      IF (t.lt.0) GO TO 120
```

```
      write(*,*) 'thinking'
      T = t * .025 / 300.0
      PI = 3.14159
      IF (ihd.eq.1) A = 2.0 / (1.+ 207.*.511/938.)
      IF (ihd.eq.2) A = 2.0 / (1.+ 207.*.511/2./938.)
      AP1 = (A+1.)
      AP1S = AP1 * AP1
      AM1 = (A-1.)
      AM1S = AM1 * AM1
      ALFA = AM1S/AP1S
      ASP1 = A*A + 1.
      ASM1 = A*A - 1.
      AAM1 = A*(A-1.)
      AAP1 = A*(A+1.)
      AD = (A-1.)/A
      APD = (A+1.)/A
      ADM = A / (A-1.)
      Q = .183
      v1eV = 3. * SQRT(2./9.38) * .001
      v0 = DSQRT(E0/a) * v1eV
C               ***************  INITIAL CONDITION  **************
c                           write(*,*)'initial condition'
      SLAST0 = 0.
      TLAST0 = 0.
      DO 42 IP=1,NN
        psis0(ip) = 0.
        psit0(ip) = 0.
        qst(ip) = -.049
        qts(ip) = .049
        IF (ihd.eq.1) READ(11,*) QST(IP), QTS(IP)
        FIS0(1,IP) = PSIS0(IP) * DSQRT(E(IP))
        FIT0(1,IP) = PSIT0(IP) * DSQRT(E(IP))
        SLAST0 = SLAST0 + PSIS0(IP)
        TLAST0 = TLAST0 + PSIT0(IP)
42    CONTINUE
      ANG = 2./3./A
      DO 11 I=1,NN
        READ(12,*) ANGST(I), ANGTS(I)
11    CONTINUE
C                     **********  INITIALIZE SIGMAS   ********
c                           write(*,*)'initialize sigmas'
      DO 10 I=1,NN
        E(i) = real(i) / 20.
        DE = E(NN) / FLOAT(NN)
        IF (ihd.eq.1) read(21,*) sigss(i),sigst(i),sigts(i),sigtt(i)
        IF (ihd.eq.2) read(20,*) sigss(i),sigst(i),sigts(i),sigtt(i)
        XMOLEC = (1.2 + .488 * t / E(I) ) * 2.0
        SIGSS(I) = XMOLEC * SIGSS(I) * press * .25
        SIGST(I) = XMOLEC * SIGST(I) * press * .25
        SIGTS(I) = XMOLEC * SIGTS(I) * press * .25
        SIGTT(I) = XMOLEC * SIGTT(I) * press * .25
        SIGS(I) = SIGSS(I) + SIGST(I)
        SIGT(I) = SIGTS(I) + SIGTT(I)
        EPH(I) = A * SQRT(E(I) + APD*QTS(I)) + SQRT(E(I))
        EPH(I) = EPH(I)*EPH(I) / AP1S
        EPL(I) = A * SQRT(E(I) + APD*QTS(I)) - SQRT(E(I))
        EPL(I) = EPL(I)*EPL(I) / AP1S
        IF (E(I).LT.APD*QST(I)) GO TO 16
        EMH(I) = A * SQRT(E(I) - APD*QST(I)) + SQRT(E(I))
        EMH(I) = EMH(I)*EMH(I) / AP1S
        EML(I) = A * SQRT(E(I) - APD*QST(I)) - SQRT(E(I))
```

```
      EML(I) = EML(I)*EML(I) / AP1S
      GO TO 18
16     EML(I) = -1.
      EMH(I) = -1.
18     CONTINUE
C  DIFFUSION VECTORS
      DIFSS(I) = SIGT(I) - SIGTT(I)*ANG
      DIFTT(I) = SIGS(I) - SIGSS(I)*ANG
      DIFTS(I) = SIGTS(I)*ANGTS(I)
      DIFST(I) = SIGST(I)*ANGST(I)
      DET = DIFSS(I)*DIFTT(I) - DIFST(I)*DIFTS(I)
      IF (DET.LT.0.0001) WRITE(*,*) 'DET = ',DET
      DIFSS(I) = DIFSS(I)/(3.0*DET)
      DIFST(I) = DIFST(I)/(3.0*DET)
      DIFTS(I) = DIFTS(I)/(3.0*DET)
      DIFTT(I) = DIFTT(I)/(3.0*DET)
10   CONTINUE
     sig0ss = sigint(sigss,e0)
     sig0st = sigint(sigst,e0)
     sig0ts = sigint(sigts,e0)
     sig0tt = sigint(sigtt,e0)
     sig0s = sig0ss + sig0st
     sig0t = sig0ts + sig0tt
     IF (ihd.eq.1) dprime = d + 2. / sigss(1)
     IF (ihd.eq.2) dprime = d + 4. / (sigs(1)+sigt(1))
     write(*,*) 'extrapolated width = ',dprime, 'cm  compared to',d
     DO 5 I=1,NN
     B(I) = FLOAT(2*I-1) * PI / Dprime
C    B(I) = 0.
 5   CONTINUE
     write(*,*) fac1*totunc(sig0s*d) + fac2*totunc(sig0t*d),
    c              '% escapes uncollided'
     write(*,*) 100.*totunc(sig0s*d),'% of singlet escapes uncollided'
     write(*,*) 100.*totunc(sig0t*d),'% of triplet escapes uncollided'
C    KERNELS - MATRICES
     DO 20 I = 1,NN
     DO 30 IP = 1,NN
     DOWN = DMAX1(E(I) - .5*DE, E(IP)*ALFA)
     IF (I.EQ.1) DOWN = DMAX1(0.D+00, E(IP)*ALFA)
     UP = DMIN1(E(I) + .5*DE, E(IP))
     FAC = SDIN(E(IP),E(I), 0.00001)
     PSS(I,IP) = FAC * SIGSS(IP) * (UP-DOWN)
     IF (DOWN.GE.UP) PSS(I,IP) = 0.
     PTT(I,IP) = FAC * SIGTT(IP) * (UP-DOWN)
     IF (DOWN.GE.UP) PTT(I,IP) = 0.
C    INELASTIC  S - T
     DOWN = DMAX1(E(I) - .5*DE, EML(IP))
     IF (I.EQ.1) DOWN = DMAX1(0.D+00, EML(IP))
     UP = DMIN1(E(I) + .5*DE, EMH(IP))
     IF (DOWN.GE.UP) GO TO 22
     FAC = SDIN(E(IP), E(I), -QST(IP))
     PST(I,IP) = FAC * SIGST(IP) * (UP-DOWN)
     GO TO 24
22   PST(I,IP) = 0.
24   CONTINUE
C    INELASTIC  T - S
     DOWN = DMAX1(E(I) - .5*DE, EPL(IP))
     IF (I.EQ.1) DOWN = DMAX1(0.D+00, EPL(IP))
     UP = DMIN1(E(I) + .5*DE, EPH(IP))
     IF (I.EQ.NN) UP = DMIN1(E(I)+1000., EPH(IP))
     FAC = SDIN(E(IP), E(I), QTS(IP))
```

```
      PTS(I,IP) = FAC * SIGTS(IP) * (UP-DOWN)
      IF (DOWN.GE.UP) PTS(I,IP) = 0.
30    CONTINUE
20    CONTINUE
c                              write(*,*)'end kernels - matrices'
      rsumel = 0.
      rsumst = 0.
      rsumts = 0.
      DO 40 i = 1,nn
        ratioel(i) = sdin(e0, e(i), 0.)
        ratiost(i) = sdin(e0, e(i), -qst(nn))
        ratiots(i) = sdin(e0, e(i), qts(nn))
        rsumel = rsumel + ratioel(i)
        rsumst = rsumst + ratiost(i)
        rsumts = rsumts + ratiots(i)
40    CONTINUE
      DO 45 i = 1,nn
        ratioel(i) = ratioel(i) / rsumel
        ratiost(i) = ratiost(i) / rsumst
        ratiots(i) = ratiots(i) / rsumts
c       write(*,*) ratioel(i), ratiost(i), ratiots(i)
45    CONTINUE
      DO 52 IP = 1,NN
      SIGSS(IP) = 0.
      SIGST(IP) = 0.
      SIGTS(IP) = 0.
      SIGTT(IP) = 0.
      DO 54 I = 1,NN
      SIGSS(IP) = SIGSS(IP) + PSS(I,IP)
      SIGST(IP) = SIGST(IP) + PST(I,IP)
      SIGTS(IP) = SIGTS(IP) + PTS(I,IP)
      SIGTT(IP) = SIGTT(IP) + PTT(I,IP)
54    CONTINUE
      SIGS(IP) = SIGSS(IP) + SIGST(IP)
      SIGT(IP) = SIGTS(IP) + SIGTT(IP)
C     WRITE(3,3) SIGSS(IP), SIGST(IP), SIGTS(IP), SIGTT(IP)
52    CONTINUE
C     ************************  TIME EVOLUTION  ******************
c                                write(*,*)'evolution'
      KEND = 0
      DO 100 NF = 1,NFMAX
      DO 70 I = 1,NN
        PSIS(I) = 0.
        PSIT(I) = 0.
        FIS(1,I) = 0.
        FIT(1,I) = 0.
70    CONTINUE
      SLAST = 0.
      TLAST = 0.
      L1 = 1
      L2 = 2
      sos = 1.
      K = 0
c                                write(*,*)'time loop starts'
50    CONTINUE
C                             *******  TIME LOOP STARTS  ********
      K = K + 1
      t = dt * float(k)
      NUL = MOD(K,nplot)
      STOT = 0.
      TTOT = 0.
```

```
      SJUNK = 0.
      TJUNK = 0.
      EAVS = 0.
      EAVT = 0.
      DO 60 I=1,NN
        FIS(L2,I) = 0.
        FIT(L2,I) = 0.
        DO 65 IP=1,NN
      FIS(L2,I) = FIS(L2,I) + PSS(I,IP)*FIS(L1,IP)+PTS(I,IP)*FIT(L1,IP)
      FIT(L2,I) = FIT(L2,I) + PST(I,IP)*FIS(L1,IP)+PTT(I,IP)*FIT(L1,IP)
65     CONTINUE
      FIS(L2,I) = FIS(L2,I) - SIGS(I)*FIS(L1,I) - b(nf)*b(nf)*
     c            (difss(i)*fis(l1,i) + difts(i)*fit(l1,i))
      FIT(L2,I) = FIT(L2,I) - SIGT(I)*FIT(L1,I) - b(nf)*b(nf)*
     c            (difst(i)*fis(l1,i) + diftt(i)*fit(l1,i))
      FIS(L2,I) = FIS(L2,I) * DT * DSQRT(E(I)) * v1eV  + FIS(L1,I)
      FIT(L2,I) = FIT(L2,I) * DT * DSQRT(E(I)) * v1eV  + FIT(L1,I)
      IF (100.*(sos+sot).lt.0.0000001) GO TO 90
        sos=(source(nf,v0,t,d,sig0s)+source(nf,v0,t+dt,d,sig0s))/2.
        sot=(source(nf,v0,t,d,sig0t)+source(nf,v0,t+dt,d,sig0t))/2.
        DO 80 is=1,ns-1
          tprime = t + float(is)*dt/float(ns)
          sos = sos + source(nf,v0,tprime,d,sig0s)
          sot = sot + source(nf,v0,tprime,d,sig0t)
 80     CONTINUE
        sos = sos / float(ns)
        sot = sot / float(ns)
      fis(l2,i) = fis(l2,i) + DT * DSQRT(E(I)) * ratioel(i) *
     c            v0 * sig0ss * fac1 * sos
      fis(l2,i) = fis(l2,i) + DT * DSQRT(E(I)) * ratiots(i) *
     c            v0 * sig0ts * fac2 * sot
      fit(l2,i) = fit(l2,i) + DT * DSQRT(E(I)) * ratiost(i) *
     c            v0 * sig0st * fac1 * sos
      fit(l2,i) = fit(l2,i) + DT * DSQRT(E(I)) * ratioel(i) *
     c            v0 * sig0tt * fac2 * sot
 90    CONTINUE
      PSIS(I) = FIS(L2,I) / DSQRT(E(I))
      PSIT(I) = FIT(L2,I) / DSQRT(E(I))
      STOT = STOT + PSIS(I)
      TTOT = TTOT + PSIT(I)
      SJUNK = SJUNK + SIGTS(I) * FIT(L1,I) - SIGST(I) * FIS(L1,I)
    SJUNK = SJUNK-B(NF)*B(NF)*(DIFSS(I)*FIS(L1,I)+DIFTS(I)*FIT(L1,I))
      TJUNK = TJUNK - SIGTS(I) * FIT(L1,I) + SIGST(I) * FIS(L1,I)
    TJUNK = TJUNK-B(NF)*B(NF)*(DIFST(I)*FIS(L1,I)+DIFTT(I)*FIT(L1,I))
      CHECK = STOT + TTOT
 60  CONTINUE
    FRESHS = SLAST-STOT + v0*sig0ss*fac1*sos*
   c     dt + v0 * sig0ts * fac2*sot*dt
    FRESHT = TLAST-TTOT + v0*sig0st*fac1*sos*
   c    dt + v0 * sig0tt * fac2*sot*dt
      FRESH = FRESHS + FRESHT
    WRITE(NF,1)DT*FLOAT(K), FRESH
    OUTS(K) = OUTS(K) + FRESHS / dt
    OUTT(K) = OUTT(K) + FRESHT / dt
    OUT(K) = OUT(K) + fresh / DT
    SLEFT(K) = SLEFT(K) + STOT
    TLEFT(K) = TLEFT(K) + TTOT
C    WRITE(3,1)STOT,TTOT, (STOT-SLAST)/DT, SJUNK, (TTOT-TLAST)/DT,TJUNK
    IF (CHECK.LT.0.0) WRITE(*,*) ' NO. INSIDE IS NEGATIVE, TIME = ',
    C           K * DT
    IF (CHECK.LT.0.0) GOTO 99
```

```
      SLAST = STOT
      TLAST = TTOT
c     IF (NUL.NE.0) GO TO 62
C     WRITE(1,1) E(NN), 0.0, 0.0
C     WRITE(1,1) E(1), 0.0, 0.0
C     WRITE(1,1)
c62   CONTINUE
      L3 = L2
      L2 = L1
      L1 = L3
      IF ((CHECK.GE.ENOUGH).AND.(K.LE.KMAX)) GOTO 50
      KEND = MAX(K,KEND)
99    CONTINUE
100   CONTINUE
C                        ******** END EVOLUTION  ***********
c                             write(*,*)'end evolution'
C     OUTS(1) = OUTS(1) + REST * SLAST0
C     OUTT(1) = OUTT(1) + REST * TLAST0
C     OUT(1) = OUTS(1) + OUTT(1)
      DO 110 K = 1,KEND
        IF (nul.ne.0) GO TO 111
c         WRITE(8,1) DT*K,OUT(K),SLEFT(K),TLEFT(K),SLEFT(K) + TLEFT(K)
111   CONTINUE
110   CONTINUE
      DO 115 K = 1,KEND
        IF (nul.ne.0) GO TO 116
        uncs = uncol(v0, dt*k, d, sig0s) * fac1
        unct = uncol(v0, dt*k, d, sig0t) * fac2
c       WRITE(8,1) DT*K, uncs + unct, uncs,unct
116   CONTINUE
115   CONTINUE
      DO 117 K = 1,KEND
        IF (nul.ne.0) GO TO 118
        uncs = uncol(v0, dt*k, d, sig0s) * fac1
        unct = uncol(v0, dt*k, d, sig0t) * fac2
        WRITE(8,1) DT*K, out(k) + uncs + unct
118   CONTINUE
117   CONTINUE
120   CONTINUE
      STOP
      END
C     ***************** ERFC ************************
      FUNCTION ERFC(X)
      IMPLICIT REAL*8(A-H,O-Z)
      Z = ABS(X)
      T = 1. / (1. + .5 * Z)
      ERFC = T * EXP(-Z*Z - 1.26551223 + T * (1.00002368 + T *
     C      (.37409196 + T * (.09678418 + T * (-.18628806 + T *
     C      (.278868077 + T * (-1.13520398 + T * (1.48851587 + T *
     C      (-.82215223 + T * .17087277)))))))))
      IF (X.LT.0.) ERFC = 2. - ERFC
      RETURN
      END
C     ***************** ERF ************************
      FUNCTION ERF(X)
      IMPLICIT REAL*8(A-H,O-Z)
      ERF = 1. - ERFC(X)
      RETURN
      END
C     ***************** SDIN ************************
      FUNCTION SDIN(EP,E,Q)
```

```
      IMPLICIT REAL*8(A-H,O-Z)
      COMMON /SMALL/ A, T
      IF (T.gt..01) GO TO 20
        sdin = st0(ep,e,q)
        RETURN
   20 CONTINUE
      A5 = SQRT(A)
      QT = Q / T
      ET = E / T
      EPT = EP / T
      AP1S = (A + 1.) * (A + 1.)
      BETA = 1. + (A+1.)/A * Q / EP
      IF (BETA.LE.0.0) GO TO 10
      BETA = SQRT (BETA)
      X = (SQRT(EPT) + SQRT(ET)) / A5
      Y = QT + EPT - ET
      AA = (X + Y/X) / 2.
      C = (X - Y/X) / 2.
      X = ABS(SQRT(EPT) - SQRT(ET)) / A5
      IF (X.LT.0.) X = - X
      IF (X.EQ.0.) X = .00000001
      B = (X + Y/X) / 2.
      D = (X - Y/X) / 2.
      SDin = AP1S / (8. * A * EP * BETA) *
     C      ( EXP(Y) * (ERF(AA) - ERF(B)) +ERF(C) - ERF(D) )
      RETURN
   10 CONTINUE
      SDIN = 0.0
      RETURN
      END
C     ***************** St0 ************************
      FUNCTION St0(EP,E,Q)
      IMPLICIT REAL*8(A-H,O-Z)
      COMMON /SMALL/ A, T
      AP1S = (A + 1.) * (A + 1.)
      st0 = 0.
      beta = dsqrt( 1. + (a+1.)/a * q/ep )
      eplus = ep * (a*beta+1.)*(a*beta+1.) / ap1s
      eminus = ep * (a*beta-1.)*(a*beta-1.) / ap1s
      IF (e.gt.eplus) RETURN
      IF (e.lt.eminus) RETURN
      St0 = ap1s / (4. * a * dsqrt(ep*ep + (a+1.)/a*q*ep) )
      RETURN
      END
      FUNCTION sigint(sig,e)
c                                              **********
c     interpolates in energy - for sig               * sigint *
c                                              **********
      IMPLICIT REAL*8(A-H,O-Z)
      DIMENSION sig(20)
c     write(*,*) '                    sigint'
c     write(*,*) e
      ee = e
      IF (ee.lt.0.05) ee = .05
      IF (ee.gt.1.0) ee = 1.0
      iec = int(ee/0.05)
      ied = iec + 1
      c = 0.05 * float(iec)
      d = 0.05 * float(ied)
      z = (d-ee) * sig(iec) + (ee-c) * sig(ied)
      sigint = z / 0.05
```

```
      RETURN
      END
      FUNCTION source(n,v,t,d,sigma)
c                                              *********
c                                              *source *
c                                              *********
      IMPLICIT REAL*8(A-H,O-Z)
      pi = 3.14159
      nn = 2 * n - 1
      IF (t.gt.0.) GO TO 10
        source = 8. / float(nn*nn) / pi / pi
        RETURN
 10   CONTINUE
      tau = v * t / d
      fac = 4. / float(nn*nn) / pi / pi  * exp(-v*sigma*t)
      IF (tau.lt.1.) source = fac * (1. + sin(nn*pi*tau)/(nn*pi*tau))
      IF (tau.ge.1.) source = fac / tau
      RETURN
      END
      FUNCTION uncol(v,t,d,sigma)
c                                              *********
c                                              * uncol *
c                                              *********
      IMPLICIT REAL*8(A-H,O-Z)
      IF (t.gt.0.) GO TO 10
        uncol = v / 2. / d
        RETURN
 10   CONTINUE
      tau = v * t / d
      fac = v / 2. / d  * exp(-v*sigma*t)
      IF (tau.lt.1.) uncol = fac
      IF (tau.ge.1.) uncol = fac / tau / tau
      RETURN
      END
      FUNCTION e1(x)
c                                              *********
c                                              * e1   *
c                                              *********
      IMPLICIT REAL*8(A-H,O-Z)
      IF (x.eq.0.) write(*,*) ' e1(',x,') = infinite'
      IF (x.le.1.) e1 = - log(x) - .57721566 + .99999193 * x -
     c          .24991055 * x * x + .05519968 * x * x * x -
     c    .00976004 * x * x * x * x + .00107857 * x * x * x * x * x
      IF (x.gt.1.) e1 = exp(-x) / x * (x*x + 2.334733*x + .250621) /
     c          (x*x + 3.330657*x + 1.681534)
      RETURN
      END
      FUNCTION e2(x)
c                                              *********
c                                              * e2   *
c                                              *********
      IMPLICIT REAL*8(A-H,O-Z)
      IF (x.gt.0.) GO TO 10
        e2 = 1.
        RETURN
 10   CONTINUE
      e2 = exp(-x) - x * e1(x)
      RETURN
      END
      FUNCTION totunc(x)
c                                              *********
```

```
c                                                    *totunc *
c                                                    *********
      IMPLICIT REAL*8(A-H,O-Z)
      IF (x.gt.0.) GO TO 10
        totunc = 1.
        RETURN
   10 CONTINUE
      totunc = ( (1. - exp(-x)) / x  +  e2(x) ) / 2.
      RETURN
      END
c
c                       program THIN
c
    1 FORMAT(5(f12.6))
      call exper
      a = 2.
  100 CONTINUE
        write(*,*) ' E0 = ? eV'
        read(*,*) e0
        IF (e0.lt.0.) GO TO 110
        v = 3. * sqrt(2.*e0/9.38/a) * .001
        call deut(v)
        GO TO 100
  110 CONTINUE
c     write(*,*) ' hydrogen = 1      deuterium = 2'
c     read(*,*) i
c     IF (i.eq.1) call hydro(v)
c     IF (i.eq.2) call deut(v)
c     d = .09 * 2.54
c     p = .188
c     d = 1.
c     p = 1.
c     sigma = .25 * 20 * p
c     sigma = 100.
c     sigma = 2.4 * sigma
c     write(*,*) 'sigma * d = ', sigma*d
c     write(*,*) 'total uncollided = ', totunc(sigma*d)
c     sum1 = 0.
c     sum0 = 0.
c     DO 10 i=1,1001
c       t = float(i-1)
c       y = v * sigma * source(1,v,t,d,sigma)
c       sum1 = sum1 + y
c       write(1,1) t, y
c 10  CONTINUE
c     write(*,*) 'sum0 = ', sum0, '   sum1 = ', sum1
c     write(*,*) 'left in 1st mode ', source(1,v,1000.,d,sigma)
      STOP
      END
      SUBROUTINE hydro(v)
c                                                    *********
c                                                    * hydro *
c                                                    *********
    1 FORMAT(5(f12.6))
```

```
      d = .09 * 2.54
      p = .188
      sigss = .25 * 5. * p * 2.4
      sigst = .25 * 70. * p *2.4
      sigts = .25 * 25. * p *2.4
      sigtt = .25 * 100. * p *2.4
      sigs = sigss + sigst
      sigt = sigts + sigtt
      write(*,*) 'sigmas * d = ', sigs*d
      write(*,*) 'sigmat * d = ', sigt*d
      write(*,*) 'singlet uncollided = ', totunc(sigs*d) * .25
      write(*,*) 'triplet uncollided = ', totunc(sigt*d) * .75
      sum1 = 0.
      sum0 = 0.
      DO 10 i=1,501
        t = float(i-1)
        y = uncol(v,t,d,sigt) * .75
        sum1 = sum1 + y
        write(1,1) t, y
   10 CONTINUE
      DO 20 i=1,501
        t = float(i-1)
        y = uncol(v,t,d,sigs) * .25
        sum0 = sum0 + y
        write(1,1) t, y
   20 CONTINUE
      write(*,*) 'sum0 = ', sum0, '  sum1 = ', sum1
      write(*,*) 'left in 1st mode ', source(1,v,1000.,d,sigs) * .25
      write(*,*) 'left in 1st mode ', source(1,v,1000.,d,sigt) * .75
      DO 30 i=1,501
        t = float(i-1)
        write(1,1) t, uncol(v,t,d,sigs)*.25 + uncol(v,t,d,sigt)*.75
   30 CONTINUE
      RETURN
      END
      SUBROUTINE exper
c                                                  *********
c                                                  * exper *
c                                                  *********
    1 FORMAT(5(f12.6))
      x = .00075/250.
      write(1,1) 190., 610.*x
      write(1,1) 230., 540.*x
      write(1,1) 270., 450.*x
      write(1,1) 310., 400.*x
      write(1,1) 350., 340.*x
      write(1,1) 390., 280.*x
      write(1,1) 450., 230.*x
      write(1,1) 520., 160.*x
      write(1,1) 600., 130.*x
      write(1,1) 680., 100.*x
      write(1,1) 760., 90.*x
      write(1,1) 840., 60.*x
      write(1,1) 920., 50.*x
      write(1,1) 1000., 50.*x
      RETURN
      END
      SUBROUTINE deut(v)
c                                                  *********
c                                                  * deut  *
c                                                  *********
```

```
 1  FORMAT(5(f12.6))
    d = .09 * 2.54
    p = .188
    write(*,*) 'd = ? in'
    read(*,*) d
    d = d * 2.54
    write(*,*) 'p = ? bar'
    read(*,*) p
    sigma = .25 * 20 * p
    sigma = 2.4 * sigma
    write(*,*) 'sigma * d = ', sigma*d
    write(*,*) 'total uncollided = ', totunc(sigma*d)
    sum1 = 0.
    sum0 = 0.
    DO 10 i=1,1001
      t = float(i-1)
      y = colfi1(d/2.,v,t,d,sigma)
      sum1 = sum1 + y
c     write(1,1) t, y
 10 CONTINUE
    DO 20 i=1,1001
      t = float(i-1)
      y = uncol(v,t,d,sigma)
      sum0 = sum0 + y
c     write(1,1) t, y
 20 CONTINUE
    write(*,*) 'sum0 = ', sum0, '  sum1 = ', sum1
    write(*,*) 'left in 1st mode ', source(1,v,1000.,d,sigma)
    DO 30 i=1,1001
      t = float(i-1)
      write(1,1) t, colfi1(d/2.,v,t,d,sigma) + uncol(v,t,d,sigma)
 30 CONTINUE
    RETURN
    END
    FUNCTION source(n,v,t,d,sigma)
c                                          *********
c                                          *source *
c                                          *********
    pi = 3.14159
    nn = 2 * n - 1
    IF (t.gt.0.) GO TO 10
      source = 8. / float(nn*nn) / pi / pi
      RETURN
 10 CONTINUE
    tau = v * t / d
    fac = 4. / float(nn*nn) / pi / pi  * exp(-v*sigma*t)
    IF (tau.lt.1.) source = fac * (1. + sin(nn*pi*tau)/(nn*pi*tau))
    IF (tau.ge.1.) source = fac / tau
    RETURN
    END
    FUNCTION colfi1(x,v,t,d,sigma)
c                                          *********
c                                          *colfi1 *
c                                          *********
    n = 10
    sum = angcol(x,1.,v,t,d,sigma) / 2.
    DO 20 i=1,n-1
      angi = float(i) / float(n)
      sum = sum + angi * angcol(x,angi,v,t,d,sigma)
 20 CONTINUE
    colfi1 = sum / float(n) * 2.
```

```
      RETURN
      END
      FUNCTION angcol(x,ang,v,t,d,sigma)
c                                                  *********
c                                                  *angcol *
c                                                  *********
      a = d / 2.
      v1 = .71 * v
      sigma1 = sigma
      IF (t.gt.0.) GO TO 10
        angcol = 0.
        RETURN
   10 CONTINUE
      tt = t
      IF (ang.eq.0.) GO TO 15
        IF ( (x+a-.00000001)/ang/v .lt. t)
     c     tt = (x+a-.00000001)/ang/v
   15 CONTINUE
      n = 10
      sum = exp(-v1*sigma1*tt) * uncfi0(x-ang*v1*tt,v,t-tt,d,sigma)/2.
      sum = sum + uncfi0(x,v,t,d,sigma) / 2.
      DO 20 i = 1,n-1
        ti = tt * float(i) / float(n)
        sum = sum + exp(-v1*sigma1*ti)
     c        * uncfi0(x-ang*v1*ti,v,t-ti,d,sigma)
   20 CONTINUE
      angcol = v * sigma * sum * tt / float(n) / 2.
      RETURN
      END
      FUNCTION uncfi0(x,v,t,d,sigma)
c                                                  *********
c                                                  *uncfi0 *
c                                                  *********
      a = d / 2.
      dum = 2.
      IF (abs(x).lt.a) GO TO 10
        uncfi0 = 0.
        RETURN
   10 CONTINUE
      IF (v*t.gt.a-x) dum = dum - 1. + (a-x)/v/t
      IF (v*t.gt.a+x) dum = dum - 1. + (a+x)/v/t
      uncfi0 = dum * v / 4. / a * exp(-sigma*v*t)
      RETURN
      END
      FUNCTION uncol(v,t,d,sigma)
c                                                  *********
c                                                  * uncol *
c                                                  *********
      IF (t.gt.0.) GO TO 10
        uncol = v / 2. / d
        RETURN
   10 CONTINUE
      tau = v * t / d
      fac = v / 2. / d  * exp(-v*sigma*t)
      IF (tau.lt.1.) uncol = fac
      IF (tau.ge.1.) uncol = fac / tau / tau
      RETURN
      END
      FUNCTION e1(x)
c                                                  *********
c                                                  * e1  *
```

```
c                                                *********
      IF (x.eq.0.) write(*,*) ' e1(',x,') = infinite'
      IF (x.le.1.) e1 = - log(x) - .57721566 + .99999193 * x -
     c          .24991055 * x * x + .05519968 * x * x * x -
     c    .00976004 * x * x * x * x + .00107857 * x * x * x * x * x
      IF (x.gt.1.) e1 = exp(-x) / x * (x*x + 2.334733*x + .250621) /
     c          (x*x + 3.330657*x + 1.681534)
      RETURN
      END
      FUNCTION e2(x)
c                                                *********
c                                                * e2   *
c                                                *********
      IF (x.gt.0.) GO TO 10
        e2 = 1.
        RETURN
   10 CONTINUE
      e2 = exp(-x) - x * e1(x)
      RETURN
      END
      FUNCTION totunc(x)
c                                                *********
c                                                *totunc *
c                                                *********
      IF (x.gt.0.) GO TO 10
        totunc = 1.
        RETURN
   10 CONTINUE
      totunc = ( (1. - exp(-x)) / x  +  e2(x) ) / 2.
      RETURN
      END
```

```
C
C                 program Q
C
      IMPLICIT REAL*8(A-H,O-Z)
      DIMENSION SIG(10,10)
      DIMENSION E(10), BOLTZ(10), Q(100,2)
C
      COMMON E0, B, BK0S
C
      IORT(L) = MOD(L,2)
      JTMINF(L,J) = MIN0( IABS(L-IORT(L)-J), 1000 * IABS(L-1) )
      JTMAXF(L,J) = L + IORT(L) + J
    1 FORMAT(7(2X,F11.6))
    2 FORMAT(2X,F7.4,5(2X,E12.6))
C
C******** INITIALIZE  ************************
      KK = 20
      E0MAX = 1.
      LIMAX = 3
      N = 5
```

```
      NN = N-1
      H = 2.0 / FLOAT(N)
      A = 2.0
      B = 1.88
      THETA = 87.5
    5 CONTINUE
      WRITE(*,*) ' TEMPERATURE  = '
      READ(*,*) T
      IF (T.LE.0.0) GOTO 13
C     WRITE(11,*) ' TEMPERATURE  T = ',T
C     WRITE(11,*)
C     WRITE(11,*) '      E0      Q S->T     Q T->S   '
      Z = 0.0
      DO 7 I=0,9
        E(I+1) = .00754 * I * (I+1)
        BOLTZ(I+1) = EXP(-THETA / T * I*(I+1) )
        Z = Z + BOLTZ(I+1) * (2*I+1) * (2*IORT(I)+1)
    7 CONTINUE
C********* ENERGY LOOP **********************
      DO 510 K=1,KK
      E0 = FLOAT(K) / FLOAT(KK) * E0MAX
      RK0 = A/(A+1.) * 8.4026 * DSQRT(E0)
      DO 10 I=0,LIMAX
      DO 20 J =0,LIMAX+4
      DE = A/(A+1.) * .5323 * FLOAT(J*(J+1)-I*(I+1))
      IF (RK0*RK0.LE.DE+.0000001) GOTO 60
      RK = DSQRT( RK0*RK0 - DE )
      NJ = IABS(I-J)
   50 CONTINUE
C  ************ INTEGRAL **************
      AL = DABS(RK0-RK)
      AR = RK0+RK
      H = (AR - AL) / FLOAT(N)
      SIG(I+1,J+1) = ( AR * BES(NJ,AR) * BES(NJ,AR)
     C          + AL * BES(NJ,AL) * BES(NJ,AL) ) / 2.
      DO 30 K2=1,NN
      X = AL+FLOAT(K2)*H
      SIG(I+1,J+1) = SIG(I+1,J+1) + X * BES(NJ,X) * BES(NJ,X)
   30 CONTINUE
      SIG(I+1,J+1) = H * SIG(I+1,J+1)
      NJ = NJ + 2
      IF (NJ.LE.I+J) GOTO 50
      SIG(I+1,J+1) = FLOAT(2*J+1) * SIG(I+1,J+1) / FLOAT(2*I+1)
C***********  DONE IF < > 0  ********************
      GOTO 70
   60 CONTINUE
      SIG(I+1,J+1) = 0.0
C***********  DONE IF = 0  ********************
   70 CONTINUE
   20 CONTINUE
   10 CONTINUE
C*********  ALL INITIALIZED  ********************
C*********  ST - TS LOOP **********************
      DO 500 JSTI = 0,1
C                 WRITE(*,*) ' JSTI = ', JSTI
       JSTF = 1 - JSTI
       Q(K,JSTI+1) = 0.0
C**********  FOR ALL POSSIBLE INITIAL ROTATIONAL STATES  *********
      DO 200 LI = 0,LIMAX
C                 WRITE(*,*) ' LI = ', LI
       JTMIN = JTMINF(LI,JSTI)
```

```
      JTMAX = JTMAXF(LI,JSTI)
C********** FOR ALL POSSIBLE TOTAL ANGULAR MOMENTA *********
      DO 210 JT = JTMIN,JTMAX
C                 WRITE(*,*) ' JT = ', JT
       MULT = 2*JT + 1
       IF (JSTI.EQ.1) MULT = MULT * IMULT(LI,JT)
       LFMIN = -1
220  CONTINUE
      LFMIN = LFMIN + 1
      IF (JTMINF(LFMIN,JSTF).GT.JT) GOTO 220
      IF (JTMAXF(LFMIN,JSTF).LT.JT) GOTO 220
C****** LFMIN = OK ********************
C                 WRITE(*,*) '     LFMIN = ', LFMIN
      LFMAX = LFMIN -1
230  CONTINUE
      LFMAX = LFMAX + 1
      IF (JTMINF(LFMAX+1,JSTF).GT.JT) GOTO 240
      GOTO 230
240  CONTINUE
C****** LFMAX = OK ********************
C                 WRITE(*,*) '     LFMAX = ', LFMAX
      ZP = 0.0
      DO 250 LF = LFMIN,LFMAX
        ZP = ZP + SIG(LI+1,LF+1)
250  CONTINUE
      DO 260 LF = LFMIN,LFMAX
       Q(K,JSTI+1) = Q(K,JSTI+1) + BOLTZ(LI+1) * FLOAT(MULT) *
     C     SIG(LI+1,LF+1) / ZP * (E(LI+1) - E(LF+1))
260  CONTINUE
210  CONTINUE
200  CONTINUE
      Q(K,JSTI+1) = Q(K,JSTI+1) / Z
500  CONTINUE
510  CONTINUE
C********** WRITE **********************
      DO 520 K=1,KK
C       WRITE(11,1) FLOAT(K)/FLOAT(KK)*E0MAX, .183 - Q(K,1),
       WRITE(11,1)  .183 - Q(K,1),
     C       Q(K,2)/3. + .183
C       WRITE(*,1) FLOAT(K)/FLOAT(KK)*E0MAX, Q(K,1), Q(K,2)/3.
520  CONTINUE
C     DO 521 K=1,KK
C       WRITE(11,1) FLOAT(K)/FLOAT(KK)*E0MAX,
C   C       Q(K,2)/3. + .183
C521  CONTINUE
C      DO 522 K=1,KK
C       WRITE(11,1) FLOAT(K)/FLOAT(KK)*E0MAX, .183
C522  CONTINUE
       WRITE(11,*) ' '
       WRITE(11,*) ' '
       WRITE(11,*) ' '
C*********  ALL DONE - RETURN TO THE BEGINNING FOR NEW T *****
      GOTO 5
 13  CONTINUE
      STOP
      END
C     ***************** BESSEL ************************
      FUNCTION BES(N,X)
      IMPLICIT REAL*8(A-H,O-Z)
      IF (X.GT.3.) GOTO 30
      IF (X.LT.0.00001) GOTO 50
```

```
      Z = X * X / 2.
      Y = 1.
      T = 1.
      ITER = 5 + IFIX(SNGL(DLOG(1000.*Z + 1.)))
      DO 10 I=1,ITER
      T = - T * Z / FLOAT(I) / FLOAT(2*N+2*I+1)
      Y = Y + T
   10 CONTINUE
      DO 20 I=1,N
      Y = Y * X / FLOAT(2*I+1)
   20 CONTINUE
      BES = Y
      RETURN
   30 CONTINUE
      A = SIN(X) / X
      B = ( SIN(X) / X - COS(X) ) / X
      IF (N.GT.0) GOTO 32
      BES = A
      RETURN
   32 CONTINUE
      IF (N.GT.1) GOTO 34
      BES = B
      RETURN
   34 CONTINUE
      DO 36 I=2,N
      C = FLOAT(2*I-1) * B / X - A
      A = B
      B = C
   36 CONTINUE
      BES = C
      RETURN
   50 CONTINUE
      IF (N.EQ.0) BES=1.0
      IF (N.NE.0) BES=0.0
      RETURN
      END
C     ***************** IMULT ************************
      FUNCTION IMULT(LI,JT)
      IMULT = 1
      IF (LI.NE.1) GOTO 10
      IF (JT.EQ.2) IMULT = 2
      IF (JT.EQ.1) IMULT = 3
      RETURN
   10 IF (LI.EQ.3) IMULT = 3 - IABS(3-JT)
      RETURN
      END
```

## PART II: A FOUR GENERATION CALABI-YAU SPACE

### 1. INTRODUCTION

One of the main goals of the twentieth century theoretical physics has been the unification of all the fundamental forces in nature, the gravitational, the electromagnetic, the weak and the strong force. During the last three decades, considerable progress has been made in this direction within the framework of gauge theories. The electromagnetic and the weak interactions have been unified by Weinberg, Salam and Glashow. Grand unified theories promise to extend this model by adding the strong force, currently described by quantum chromodynamics. The gravitational force, however, does not seem to fit in such a scenario.

Another fundamental idea of this century physics is the speculation that space-time is higher-dimensional. Soon after Einstein added time to ordinary space as the fourth dimension, Kaluza and Klein proposed that electromagnetism could be described by adding a fifth dimension. This added dimension would not be directly observable, because it would be compactified into a small circle. If successful, such a theory would have unified all the forces known at that time (the weak and the strong force were discovered later) in a very elegant geometrical picture.

Superstring theories, which have caused so much excitement during the last few years, make use of both of the above ideas. They are the first theories that offer hope of unifying the gravitational force with the other three forces. In the low energy limit, they reduce to a Kaluza-Klein type gauge theory. In this theory space-time is ten

dimensional, where four dimensions are the Minkowski space-time and the additional six are compactified in a small manifold. The most promising candidates for this manifold are Calabi-Yau spaces.

A. What is a Calabi-Yau space?

According to the superstring dogma, the world in which we live is of the form $M_4 \times K_6$, where $M_4$ is the usual Minkowski space-time and $K_6$ is the compactified six dimensional Euclidean manifold.[1] One of the popular scenarios, accepted from now on in this work, is based on $K_6$ being the so called Calabi-Yau space.[1,2] This means that it is a complex (even Kähler) manifold which is Ricci flat in some (unique) metric. Since this definition may be somewhat involved, let us first explain what it amounts to and then give some examples.

Let us first recall that an n-dimensional real manifold M is a topological space, equipped with an atlas. By an atlas we mean a covering of M by open sets $U_i$, together with a set of local coordinates $\phi_i : U_i \to R^n$. The idea is simply that we want to view M locally, that is, in a patch $U_i$, as a subset of $R^n$. To explore M globally, that is, to go to another patch $U_j$, we can use the transition functions $\phi_j \circ \phi_i^{-1}$, which are defined on $\phi_i(U_i) \cap \phi_j(U_j)$. If in the above definition $R^n$ is replaced by $C^n$ and the transition functions are required to be holomorphic, we get a complex manifold. For example, the sphere $S^2$ is a complex manifold. To see this, we can cover it by two charts, $U_1 = S^2 \backslash$south pole, $U_2 = S^2 \backslash$north pole, and use stereographic projections on the planes through the south and north pole as local coordinates. The transition function $z_2 = 1/z_1$ is holomorphic, hence $S^2$ is a complex

manifold, as claimed. The condition that a manifold should be complex is nontrivial. For example, among all the spheres, $S^2$ is the only complex manifold.

On a complex manifold one can always introduce a Hermitian metric

$$ds^2 = g_{\mu\bar{\nu}}\, dz^{\mu} d\bar{z}^{\bar{\nu}} ,$$

where $\mu$ is a holomorphic and $\bar{\nu}$ an antiholomorphic index. If the metric tensor satisfies the condition

$$\partial_{\alpha} g_{\beta\bar{\gamma}} = \partial_{\beta} g_{\alpha\bar{\gamma}}$$

$$\partial_{\bar{\alpha}} g_{\bar{\beta}\gamma} = \partial_{\bar{\beta}} g_{\bar{\alpha}\gamma} ,$$

then the complex manifold is called Kähler. In a more conventional language of differential forms this simply means that the Kähler form

$$K = \frac{i}{2} g_{\mu\bar{\nu}}\, dz^{\mu} \wedge d\bar{z}^{\bar{\nu}}$$

is closed. If, moreover, we make the usual choice of no torsion, then the (Christoffel) connection simplifies to

$$\Gamma^{\bar{\gamma}}_{\alpha\beta} = \Gamma^{\gamma}_{\bar{\alpha}\beta} = 0$$

$$\Gamma^{\gamma}_{\alpha\beta} = g^{\gamma\bar{\delta}}\, \partial_{\alpha} g_{\bar{\delta}\beta} .$$

In this case the Ricci tensor takes a remarkably simple form

$$R_{\mu\bar{\nu}} = \partial_{\mu} \partial_{\bar{\nu}} \log \det g_{\alpha\bar{\beta}} .$$

The Ricci form $R = iR_{\mu\bar{\nu}}\, dz^{\mu} \wedge d\bar{z}^{\bar{\nu}}$ is always closed, but not necessarily exact (because $\det g_{\alpha\bar{\beta}}$ is not a scalar). Recalling the definition of the de Rham cohomology (closed forms modulo exact forms), we see that the Ricci form defines a cohomology class

$$c_1 = \left[ \frac{1}{2\pi} R \right] ,$$

called the first Chern class. If we equip the manifold M with another metric, then R will in general change, (but only for an exact piece), so that $c_1$ will not change. This means that the first Chern class is a topological invaiant. Obviously, if the metric is Ricci flat, then $c_1$ vanishes. It is highly nontrivial, though, that if $c_1 = 0$, there exists a (unique) Ricci flat metric. This theorem was conjectured by Calabi and proved by Yau, hence the name Calabi-Yau spaces.

Calabi-Yau spaces are characterized by the existence of a nowhere vanishing holomorphic three form

$$\Omega = \frac{1}{3!}\, \Omega_{\alpha\beta\gamma}(z) dz^{\alpha} \wedge dz^{\beta} \wedge dz^{\gamma} .$$

As an illustration, let us see how the existence of $\Omega$ implies the vanishing of the first Chern class. Within each coordinate patch $\Omega$ can be written

$$\Omega_{\alpha\beta\gamma} = f(z)\, \epsilon_{\alpha\beta\gamma} .$$

This leads to .

$$\det g_{\alpha\bar{\beta}} = \frac{3!\ |f|^2}{\bar{\Omega}^{\mu\nu\rho}\Omega_{\mu\nu\rho}} ,$$

or

$$R = -i\,\partial\bar{\partial}\,\log\,(\bar{\Omega}^{\mu\nu\rho}\Omega_{\mu\nu\rho}) ,$$

which shows that R is exact since the quantity in the bracket is by definition a globally defined scalar. The converse is much harder to prove.

B. Hodge numbers and generations of particles

A concise review of cohomology and Hodge numbers on complex manifolds is called for. Recall that for a real manifold the Betti numbers $b_i$, which count the number of linearly independent closed, nonexact (harmonic) i-forms, are topological invariants. On a complex manifold i-forms naturally decompose into (p,q) forms, p+q = i, where p and q count the number of holomorphic and antiholomorphic indices, respectively. Consequently, the Hodge numbers $h_{pq}$ count the harmonic (p,q) forms and

$$b_i = \sum_{p+q=i} h_{pq} .$$

Hodge numbers can be conveniently summarized in the Hodge diamond, which for a three dimensional complex manifold (corresponding to six real dimensions) takes the following form

$$
\begin{array}{ccccccc}
 & & & h_{33} & & & \\
 & & h_{32} & & h_{23} & & \\
 & h_{31} & & h_{22} & & h_{13} & \\
h_{30} & & h_{21} & & h_{12} & & h_{03} \\
 & h_{20} & & h_{11} & & h_{02} & \\
 & & h_{10} & & h_{01} & & \\
 & & & h_{00} & & &
\end{array}
$$

To each harmonic (p,q) form there corresponds a harmonic (3-p,3-q) form (Poincaré duality), so the Hodge diamond is symmetric about the origin. On a Kähler manifold a complex conjugate of a harmonic form is harmonic, which means that the diamond is symmetric about the vertical. Furthermore, $h_{00} = 1$, because the only harmonic function on a compact manifold is the constant function. Moreover, on a Calabi-Yau manifold, $h_{30} = 1$ due to the uniqueness of the holomorphic 3-form. It is easily seen that this implies one-one correspondence between harmonic (0,1) and (2,0) forms, which implies $h_{10} = h_{20}$. The situation further simplifies when the Euler characteristic

$$\chi_E = \sum_{p,q} (-1)^{p+q} h_{pq}$$

is nonvanishing. In that case a harmonic one-form $u_m dx^m$ satisfies the following equation on a Calabi-Yau manifold

$$\nabla^k \nabla_k u_m = 0 \ .$$

Integration by parts implies that $u_m$ is covariantly constant. But for

$\chi_E \neq 0$ $u_m$ must vanish somewhere and being covariantly constant it must vanish everywhere. Therefore the only nontrivial Hodge numbers are $h_{21}$ and $h_{11}$ and

$$\chi_E = 2(h_{11} - h_{21}) \ .$$

Moreover $h_{11}$ and $h_{21}$ have important physical meaning: they simply count the right-handed and left-handed spinors, i.e. quarks and leptons. Their difference obviously corresponds to massless fields (at least prior to Higgs induced symmetry breaking), which means that the number of generations of quarks and leptons is determined by the Euler characteristic [1,4]

$$N_g = \frac{1}{2} |\chi_E| \ . \tag{1.1}$$

Strictly speaking one has more than the usual generations of fermions, since spinors are 27 dimensional representations of E(6). Namely, the original string theory in ten dimensions has a large symmetry based on the E(8) x E(8) group, which in the four dimensional world breaks down to E(6) symmetry. Of course, the E(6) symmetry has to be broken down to the standard electroweak model symmetry $SU(3)_c$ x $SU(2)_L$ x $U(1)_{EM}$. As we shall see in Section 3, the so-called flux breaking plays a major role here. This means that we take the starting simply connected Calabi-Yau manifold based on algebraic varieties and divide it by a freely acting discrete group. The flux breaking results from the embedding of the discrete group in E(6). This, admittedly ad hoc division by a discrete group, fortunately plays an additional important role: it reduces dramatically the original Euler characteristic, which is in general too large.

C. Construction of Calabi-Yau spaces

Equipped with the definition and the above characterization of a Calabi-Yau space, let us now look for some examples. Naively, we could try complex submanifolds of $C^n$, but this does not work, because the only connected compact submanifold of $C^n$ is a point (maximum modulus principle). Next, we try the complex projective space

$$CP_n = C^{n+1} - \{0\} / \sim$$

with

$$(z_0,z_1,\ldots,z_n) \sim \lambda(z_0,z_1,\ldots,z_n), \qquad \lambda \neq 0,$$

i.e. the set of all complex lines through the origin in $C^{n+1}$. $CP_1$, for example, can be coverd with two patches, $U_1 = \{(z_0,z_1);\ z_0 \neq 0\}$ and $U_2 = \{(z_0,z_1);\ z_1 \neq 0\}$, with local coordinates

$$w_1 = \frac{z_1}{z_0} \qquad \text{and} \qquad w_2 = \frac{z_0}{z_1}$$

and transition function

$$w_2 = \frac{1}{w_1} \ ,$$

so it is just the sphere $S^2$. Now $S^2$ is not Calabi-Yau, because if it were, then its first Chern class would vanish and by the classical Gauss-Bonnet theorem the Euler characteristic would also vanish,

$$\chi_E(S^2) = \int_{S^2} c_1(S^2),$$

which we know is not true ($\chi_E(S^2) = 2$). Here we would like to stress

again the power of topological reasoning: if some property of a manifold depends only on its topology, then we can check it in any metric we want. To show that $CP_n$ is not Calabi-Yau we choose the Fubini-Study metric, in which

$$R = -i(n+1)g_{\mu\bar{\nu}}\, dz^{\mu} \wedge d\bar{z}^{\bar{\nu}} .$$

The volume form is proportional to $R \wedge R \wedge \ldots \wedge R$ (n-times) and we see that R cannot be exact, since that would imply that $CP_n$ has zero volume.

The only known systematic way of constructing Calabi-Yau spaces is as algebraic varieties, i.e. submanifolds of $CP_n$ defined by polynomial constraints. For example, take $CP_4$ with the quintic polynomial

$$z_0^5 + z_1^5 + z_2^5 + z_3^5 + z_4^5 = 0 .$$

Since, topologically speaking, only the dimension of $CP_n$ and the degree of the polynomial matter, the resulting manifold is usually denoted by $(4\|5)$. It is easy to show that the holomorphic three form

$$\frac{1}{w_4^4}\, dw_1 \wedge dw_2 \wedge dw_3 ,$$

where $w_i = z_i/z_5$, $i = 1,\ldots,4$, is nonsingular and nowhere vanishing, so that $(4\|5)$ is Calabi-Yau.

The above argument can be generalized to the case of an algebraic variety, defined by more than one polynomial. Then the resulting manifold is Calabi-Yau if and only if

$$\sum_i d_i = n + 1 ,$$

where $d_i$ is the degree of the ith polynomial. Moreover, products of projective spaces with polynomial constraints can be considered and then the above condition must hold for each $CP_n$ factor.

Remarkably, there are only a finite number of Calabi-Yau spaces that can be constructed in this manner. The reason for this is due to the fact that the linear constraint on $CP_n$ reduces it to $CP_{n-1}$. In the case of a single $CP_n$ factor this implies $n \leq 7$, since for $CP_8$ we would need a linear constraint. All in all, there are on the order of 10,000 Calabi-Yau spaces constructed in this manner.[3]

The main motivation for Calabi-Yau spaces lies in the belief in asymptotic freedom at energies below the Planck mass and N=1 supersymmetry propagating all the way into the TeV regime of weak interaction physics [4]. This immediately forbids more than four generations of quarks and leptons, and simplifies the situation dramatically. For example, only one of the thousands of these manifolds can be constructed as the three generation space--a remarkable result [3]. This is the so-called Tian-Yau manifold [5], which has been extensively studied [6,7,8]. Tian-Yau manifold is based on the following algebraic variety in $CP_3 \times CP_3$

$$\begin{bmatrix} 3 \\ 3 \end{bmatrix} \begin{Vmatrix} 3 & 0 & 1 \\ 0 & 3 & 1 \end{Vmatrix} \tag{1.2}$$

The notation of Hubsch, employed in our paper, simply implies cubic polynomials in each of the $CP_3$ spaces and a mixed polynomial linear in both the $CP_3$'s coordinates. Since its Euler characteristic $\chi_E = -18$ and, as we have seen, the number of generations $N_g = |\chi_E|/2$, one then divides

the above space by the $Z_3$ symmetry in order to obtain a multiply connected manifold with three generations [5]. It is characterized [6] by $h_{11} = 6, h_{21} = 9$ and $\chi_E = -6$. The nontrivial embedding of $Z_3$ in E(6) allows, through the so-called flux breaking [10], for the intermediate $SU(3)_L \times SU(3)_R \times SU(3)_C$ symmetry which is then broken spontaneously by the Higgs in 27 of E(6) [6].

What about the situation involving four generations? Well, we already know two explicit examples (see below) and the systematic search for these manifolds indicates there exists not too large a number [11]. However, at this point no complete analysis has been performed and we simply don't know how many of the candidate spaces could be actually constructed. Recall, the candidate manifolds are those which could allow dividing discrete symmetry free of fixed points, but only an explicit construction reveals whether this is actually achieved or not.

The existing candidates are $(4\|5)$ and $(7\|2222)$ manifolds [12], both characterized by $h_{11} = 1$, which leads to a serious problem in understanding the lightness of the neutrino [13]. These manifolds are not realistic. This fact has prompted us to search for an explicitly constructed four generation manifold with $h_{11} \neq 1$. The manifold we have constructed is in complete analogy with the Tian-Yau manifold. It is an algebraic variety $K_0$ in $CP_4 \times CP_4$ [14]

$$\begin{pmatrix} 4 & \| & 2 & 2 & 0 & 0 & 1 \\ 4 & \| & 0 & 0 & 2 & 2 & 1 \end{pmatrix} \quad , \tag{1.3}$$

with $\chi_E(K_0) = -32$. To obtain a four generation manifold K, we divide $K_0$ by a fixed point free $Z_2 \times Z_2$ symmetry. We find

(i) $h_{11}(K) = 6, \quad h_{21}(K) = 10$ ,

$$\chi_E(K) = -8 \quad . \tag{1.4}$$

(ii) the flux breaking allows the intermediate symmetry to be E(6), $SU(2)_L$ x SU(6) or, as we choose, the physically appealing Pati-Salam $SU(2)_L$ x $SU(2)_R$ x $SU(4)_C$ symmetry.

(iii) the manifold has $Z_2^2$ honest symmetry, under which we classify the transformation properties of $h_{21}$ and $h_{11}$ fields and in turn quarks and leptons.

The rest of the work is devoted to the detailed analysis of this manifold. We follow the pedagogical and systematic procedure of Greene et al. In the next section we present the manifold and compute its Hodge numbers and the Euler characteristic. We then demonstrate that the $Z_2$ x $Z_2$ dividing symmetry is freely acting, but leave the nontrivial and tedious part of the transversality of our polynomial constraints for the Appendix.

Section 3 concerns the flux breaking and it is there where the physical fields are identified. Their transformation properties under the honest symmetry are computed in section 4. Finally, in section 5 we give concluding remarks and offer some thoughts regarding the phenomenological consequences.

## 2. A FOUR GENERATION MANIFOLD: THE CONSTRUCTION

### A. The simply connected manifold $K_0$

As we said in the introduction, the manifold is based on an algebraic variety $K_0$ in $CP_4 \times CP_4$ with the most general polynomials

$$P_1 = \frac{1}{2} \sum_{i=0}^{4} x_i^2 = 0$$

$$P_2 = \frac{1}{2} \sum_{i=0}^{4} a_i x_i^2 = 0$$

$$P_3 = \sum_{i,j=0}^{4} c_{ij} x_i y_j = 0$$

$$P_4 = \frac{1}{2} \sum_{i=0}^{4} b_i y_i^2 = 0$$

$$P_5 = \frac{1}{2} \sum_{i=0}^{4} y_i^2 = 0 \quad , \tag{2.1}$$

where $x_i$ and $y_i$ are the homogenous coordinates on the two $CP_4$'s and $a_i$, $b_i$, $c_{ij}$ are in general complex parameters (of course, you can always choose $a_0 = b_0 = c_{00} = 1$. We have used the freedom in linear redefinitions of the coordinates on the $CP_4$'s to simultaneously diagonalize the quadratics $P_1, P_2$ and $P_3, P_4$. Of course, (2.1) will not make sense for just any choice of these parameters; in order for it to define a smooth manifold the above polynomials must be transverse [16], i.e. $dP_1 \wedge dP_2 \wedge dP_3 \wedge dP_4 \wedge dP_5$ is not allowed to vanish on $K_0$. The tedious, but important, computation which establishes the transversality is given in the Appendix; it leads to a number of involved constraints on

$a_i$, $b_i$ and $c_{ij}$. We now turn our attention to topological properties of $K_0$.

Hodge numbers of $K_0$

$K_0$ is a Calabi-Yau manifold with SU(3) holonomy. This implies $h_{20} = h_{10} = 0$, $h_{30} = 1$ and the only nontrivial Hodge numbers are given by $h_{21}$ and $h_{11}$ [1,2]. They simply count chiral fermionic zero modes on the manifold, with $h_{21}$ counting the 27's of E(6) and $h_{11}$ counting the $\overline{27}$'s. This guarantees $h_{21} - h_{11}$ light families, which cannot be paired off above $M_W$ scale; hence the number of generations is [1]

$$N_g = h_{21} - h_{11} = -\frac{1}{2}\chi_E \quad . \tag{2.2}$$

i) $h_{21}$ and the deformations of the polynomials

It is well known that, except in some strange instances [17], $h_{21}$ is given by small deformations of $K_0$, i.e. small deformations of the polynomials. In other words, to each closed, non-exact (2,1) form corresponds an independent deformation of $P_i$. Independent deformations are simply those which are unrelated by linear analytic coordinate transformations. This is neatly summarized by Candelas [18]: a deformation vanishes effectively (i.e. it corresponds to an exact form), if it is proportional to any of $P_i$ or their derivatives:

$$z_i \frac{\partial P^\alpha}{\partial z_j} + \sum_\beta f^\alpha_\beta P^\beta \simeq 0 \quad , \tag{2.3}$$

where $z_i$ are either of the two $CP_4$'s homogeneous coordinates $x_i$ and $y_i$,

$\alpha = 1,\ldots,5$ and $f^{\alpha}_{\beta}$ are arbitrary parameters. Let us see how this works on our manifold. First, there are altogether 85 possible deformations of polynomials $P_i$; they are of the form: $x_ix_j$, $y_iy_j$, $x_iy_j$. Now, let $f^{\alpha}_{\beta} = 0$ in (2.3); in vector notation $z_i = x_i$ in (2.3) gives

$$\begin{pmatrix} x_ix_j \\ x_ia_jx_j \\ \Sigma_k x_ic_{jk}y_k \\ 0 \\ 0 \end{pmatrix} \simeq 0 \quad . \tag{2.4}$$

This means that the deformations of say $P_1$ (and similarly $P_5$) are determined by the deformations of $P_2$, $P_3$ and $P_4$. Antisymmetrizing (2.4) gives in turn

$$\begin{pmatrix} 0 \\ (a_j - a_i)x_ix_j \\ \Sigma_k(x_ic_{jk} - x_jc_{ik})y_k \\ 0 \\ 0 \end{pmatrix} \simeq 0 \quad , \tag{2.5}$$

which tells us similarly that the off-diagonal deformations of $P_2$ (and also $P_4$) are not independent of the others. On the other hand, $f^{\alpha}_{\beta} \neq 0$ amounts to saying that we can use both $\Sigma_i x_i^2 = 0$ and $\Sigma_i a_i x_i^2 = 0$ for (now only diagonal) deformations of $P_2$ (and $P_4$). But since

$$\sum_i a_i x_i \frac{\partial \vec{P}}{\partial x_i} = \begin{pmatrix} 0 \\ \Sigma_i a_i^2 x_i^2 \\ \Sigma_{i,k} a_i x_i c_{ik} y_k \\ 0 \\ 0 \end{pmatrix} \simeq 0 \quad , \tag{2.6}$$

one more diagonal deformation of $P_2$ (and $P_4$) can be traded for $P_3$ deformations.

In summary, we are left at the end with 2 diagonal deformations of $P_2$ and $P_4$ each and 25-1 (use $P_3 = 0$) = 24 independent deformations of $P_3$. This shows that

$$h_{21}(K_0) = 28 \quad . \tag{2.7}$$

The choice of the deformations we found convenient will be displayed later, when we discuss their transformation properties under the dividing symmetry.

ii) $h_{11}$ and the Lefschetz hyperplane theorem

Since the Euler characteristic of this manifold is independently known, we could simply use $h_{11} = h_{21} + \chi_E/2$ from (2.2). However, in order to verify the deformation method and our computations we will evaluate $h_{11}$ directly, using the Lefschetz hyperplane theorem. This theorem asserts that $h_{11}(K_0)$ is simply the sum of the corresponding Hodge numbers of the submanifolds obtained by ignoring the mixed polynomial(s) [19]. In our case this reads as

$$h_{11}(K_0) = 2\, h_{11}(U), \tag{2.8}$$

where U=(4‖22). From $\chi_E(U)=8$, $h_{11}(U)=6$ and so

$$h_{11}(K_0) = 12. \tag{2.9}$$

B. The four generation manifold K

Since $\chi_E(K_0)=-32$, we need a four element dividing group to obtain a four generation manifold. It is easy to see that the choice $c_{ij}$ diagonal, i.e.

$$\begin{aligned} P_1 &= \frac{1}{2} \sum_{i=0}^{4} x_i^2 = 0 \\ P_2 &= \frac{1}{2} \sum_{i=0}^{4} a_i x_i^2 = 0 \\ P_3 &= \sum_{i=0}^{4} c_i x_i y_i = 0 \\ P_4 &= \frac{1}{2} \sum_{i=0}^{4} a_i y_i^2 = 0 \\ P_5 &= \frac{1}{2} \sum_{i=0}^{4} y_i^2 = 0 \end{aligned} \tag{2.10}$$

gives rise to a $Z_2^5$ symmetry of $K_0$ (see section 4).

Notice that we have now assumed the swapping symmetry x <-> y. This calls for a $Z_2$ x $Z_2$ dividing symmetry, which up to reshuffling of the coordinates, is uniquely given by

$$g_1 = \text{diag } (1,1,1,-1,-1), \; g_2 = \text{diag } (1,1,-1,1,-1) \; . \tag{2.11}$$

For K to be a smooth manifold, $Z_2$ x $Z_2$ must act freely [1]. Let us see how this works for $g_1$, in which case the fixed point equation is

$$(x_0,x_1,x_2,x_3,x_4) \to (x_0,x_1,x_2,-x_3,-x_4) = \lambda(x_0,x_1,x_2,x_3,x_4)$$

$$(y_0,y_1,y_2,y_3,y_4) \to (y_0,y_1,y_2,-y_3,-y_4) = \lambda'(y_0,y_1,y_2,y_3,y_4) \ , \quad (2.12)$$

where $\lambda$ and $\lambda'$ are nonzero complex numbers. Eq. (2.12) implies $\lambda = -1$ or $\lambda = 1$, of which the first case obviously gives no solution. The $\lambda = 1$ case requires a little care. It implies $x_3 = x_4 = y_3 = y_4 = 0$ and so from (2.10) we get

$$x_0^2 + x_1^2 + x_2^2 = 0, \qquad y_0^2 + y_1^2 + y_2^2 = 0$$

$$a_0x_0^2 + a_1x_1^2 + a_2x_2^2 = 0, \qquad a_0y_0^2 + a_1y_1^2 + a_2y_2^2 = 0$$

$$c_0x_0y_0 + c_1x_1y_1 + c_2x_2y_2 = 0 \quad . \qquad (2.13)$$

Solving for the $x_1$, $x_2$, $y_1$ and $y_2$ from the first four equations implies

$$c_0x_0y_0 + c_1x_1y_1 + c_2x_2y_2 =$$

$$= \{ \frac{1}{a_2 - a_1} [c_0(a_1 - a_2) \pm c_1(a_2-a_0) \pm c_2(a_0-a_1)]\}x_0y_0 = 0 \quad . \qquad (2.14)$$

Assuming that the expression in the bracket does not vanish (see also the Appendix), $x_0 = 0$ and (2.13) has no solution. In exactly the same manner one can check that $g_2$ and $g_1g_2$ have no fixed points.

The fact that $G_F$ acts freely means that K is a smooth manifold whose Euler characteristic is determined through $\chi_E(K_0)$ [1]

$$\chi_E(K) = \frac{\chi_E(K_0)}{\#\text{ of elements of } G_F} = \frac{-32}{4} = -8 \ . \qquad (2.15)$$

In other words, K, as promised, is a four generation manifold. This will be even more manifest when we display its Hodge numbers below.

Hodge numbers of K

i) $h_{21}$

As we said in A, we choose the 28 independent deformations of $K_0$ to be 2 diagonal for each $P_2$ and $P_4$ and 24 for $P_3$. They are listed, together with their transformation properties under $G_F$, in Table 1. As you can see, 10 of them are invariant, which implies $h_{21}(K) = 10$.

ii) $h_{11}$

Computing $h_{11}(K)$ is somewhat more subtle and requires using the technique of Lefschetz fixed point theorem [20]. Since we lack the explicit knowledge of $h_{11}$ fields, in order to find their transformation properties we need to reconstruct the character table of $H_{11}(g_i)$ [20] under $G_F$. This is achieved through the above theorem, which asserts that for any g

$$\sum_{p,q=0}^{3} (-1)^{p+q} \, \mathrm{Tr}H_{pq}(g) = \chi(\text{fixed points of } g) \ , \qquad (2.17)$$

where the righthand side is the Euler characteristic for the fixed point submanifold of g, and $H_{pq}(g)$ is the matrix representation of g acting on $h_{pq}$ fields. Now, $g_i \epsilon G_F$ act freely and (2.17) gives

$$\mathrm{Tr}H_{11}(g_i) = \mathrm{Tr}H_{21}(g_i) \ , \qquad (2.18)$$

where we used the fact that $h_{00}$ and $h_{30}$ are invariant under $g_i$. From Table 1, (2.18) readily gives

$$\mathrm{Tr}H_{11}(g_1) = \mathrm{Tr}H_{11}(g_2) = \mathrm{Tr}H_{11}(g_1 g_2) = 4 \ ,$$

$$\mathrm{Tr}H_{11}(1) = 12 \ . \tag{2.19}$$

The number of elements $c_i$ in each of the representations $R_i$ (see Table 1) is simply given by [21]

$$c_i = \frac{1}{4} \sum_{\alpha} \mathrm{Tr}H_{11}(g_\alpha) \times g_\alpha(R_i) \ , \tag{2.20}$$

where the sum is over all the group elements of $G_F$ (recall that $G_F$ is abelian so all of its representations are one dimensional); $g_\alpha(R_i)$ is the value of $g_\alpha$ in the representation $R_i$ (Table 1). From (2.19) and (2.20)

$$\begin{aligned} c_1 &= 6 \ , \\ c_2 &= c_3 = c_4 = 2 \ . \end{aligned} \tag{2.21}$$

Since all $g_i = 1$ ($g_i \epsilon G_F$) in $R_1$, there are six invariant $h_{11}$ fields on $K_0$, i.e.

$$h_{11}(K) = 6 \ . \tag{2.22}$$

From $\chi_E(K) = 2[h_{11}(K) - h_{21}(K)] = -8$, this is yet another demonstration that K contains four light generations of quarks and leptons (actually, the full 27's of E(6)—see the next section). This manifold is a natural extension of the Tian-Yau manifold; the additional generation is obtained through the increase of $h_{21}$'s, while $h_{11}$'s are the same. The important difference and the additional motivation for our work lies in their intermediate symmetries obtained through the flux breaking. In the next section we discuss this at length and finally identify the quark and lepton fields.

3. FLUX BREAKING

It should be clear from its construction that K is a multiply connected manifold [1], with the fundamental group $\pi_1(K) = G_F$. This important feature is responsible for the badly needed breaking of E(6) gauge symmetry, through the so called flux breaking. In a sense, this justifes the otherwise ad hoc division by $G_F$ in constructing a manifold with $N_g = 4$.

Recall that in superstring compactification we lack the usually present adjoint Higgs, which is used at the first stage of symmetry breaking. Instead, the same effect is achieved via nontrivial embedding of $G_F$ in E(6)

$$g_i \to U_{g_i} \epsilon E(6) \quad . \tag{3.1}$$

For simplicity and clarity, we embed $G_F = Z_2 \times Z_2$ into $SU(2)_L \times SU(6)$ maximal subgroup of E(6)

$$\begin{aligned} U_{g1} &= \text{diag}(-1,-1) \times \text{diag}(1,1,1,1,1,1,) \\ U_{g2} &= \text{diag}(1,1) \times \text{diag}(-1,-1,1,1,1,1,) \quad , \end{aligned} \tag{3.2}$$

which implies E(6) topological breaking

$$E(6) \to SU(2)_L \times SU(2)_R \times SU(4)_C \quad . \tag{3.3}$$

The intermediate symmetry is the physically interesting case of quark-lepton unification àla Pati-Salam [22]. This can be verified through the Dynkin diagram techniques; in the notation of Slansky [23] (his Table 20) this amounts to

$$U_{g_i} = e^{i\vec{\lambda}_i \cdot \vec{H}} \quad , \tag{3.4}$$

where $\vec{H}$ covers Cartan's subalgebra and $\vec{\lambda}_i = (-c_i, c_i, a_i, b_i, c_i, 0)$ and

$$a_1 = b_1 = c_1 = \pi \quad ,$$

$$a_2 = b_2 = \pi, \quad c_2 = 0 \quad . \tag{3.5}$$

Our embedding (3.2) is clearly physically the most interesting, for otherwise the intermediate symmetry is at least $SU(2)_L \times SU(6)$.

Under $SU(2)_L \times SU(2)_R \times SU(4)_C$, 27 of E(6) decomposes in the following manner

$$27 = [(2_L, 2_R, 1_C) = \phi] + [(2_L, 1_R, 4_C) = Q_L, \psi_L] + [(1_L, 2_R, 4_C) = Q_R, \psi_R]$$

$$+ [(1_L, 1_R, 6_C) = D, D^C] + [(1_L, 1_R, 1_C) = n] \quad , \tag{3.6}$$

where besides the usual family of quarks and leptons $Q_L, Q_R$ and $\psi_L, \psi_R$, we also have new leptons $\phi$, new down quarks, D, $D^C$ and a singlet n.

Now to each 27 of E(6) (prior to flux breaking) there corresponds, as we said, a (2,1) form and to each (2,1) form an independent deformation of the defining polynomials. The fields that will remain light, i.e. those that survive the passage to K must satisfy

$$\psi(g_i x) = U_{g_i} \psi(x) \quad . \tag{3.7}$$

In the sense of the above 1-1 correspondence between physical fields and the deformations, we can write

$$\left.\begin{aligned} \phi &\simeq \tfrac{1}{2}(1-g_1)\tfrac{1}{2}(1-g_2) \\ Q_L,\psi_L &\simeq \tfrac{1}{2}(1-g_1)\tfrac{1}{2}(1+g_2) \\ Q_R,\psi_R &\simeq \tfrac{1}{2}(1+g_1)\tfrac{1}{2}(1-g_2) \\ \left.\begin{matrix} n \\ D,D^c \end{matrix}\right\} &\simeq \tfrac{1}{2}(1+g_1)\tfrac{1}{2}(1+g_2) \end{aligned}\right\} \quad \text{x deformation} \quad . \tag{3.8}$$

This simply means that n is a singlet under both $SU(2)_L$ and $SU(2)_R$; $Q_L$ a singlet under $SU(2)_R$, etc. Similarly, $\bar{\phi},\bar{Q}_L,\bar{\psi}_L,\bar{Q}_R,\bar{\psi}_R,\bar{n},\bar{D},\bar{D}^c$ are the same projections on (1,1) forms.

In Table 1 we have specified which deformations correspond to our physical fields; it tells us that the light spectrum of (2,1) forms consists of (let Q stand for $Q_L,Q_R,\psi_L,\psi_R$)

$$h_{21}: \quad 10(n + D + D^c) + 6(Q + \phi) \quad . \tag{3.9}$$

From (2.21) we find similarly that the light antiparticles on K are

$$h_{11}: \quad 6(\bar{n} + \bar{D} + \bar{D}^c) + 2(\bar{Q} + \bar{\phi}) \quad . \tag{3.10}$$

The light spectrum of the theory contains

$$\begin{aligned} &4(n + D + D^c + Q + \phi = 27) \\ &+6(n + \bar{n} + D + \bar{D} + \bar{D}^c + D^c) + 2(Q + \bar{Q} + \phi + \bar{\phi}). \end{aligned} \tag{3.11}$$

In short, besides the four 27's guaranteed by the index theorem, there are additional light particles and mirror particles whose fate will depend on the next stage of Higgs-induced symmetry breaking.

## 4. HONEST SYMMETRIES

We now discuss the ''honest'' symmetries of our four generation manifold K, i.e. the symmetries by $K_0$ that survive the division by $G_F$ and the flux breaking. We keep the general coefficients $a_i$ and $c_i$ in defining equation (2.10) of $K_0$, the manifold embedded in $CP_4 \times CP_4$. Actually, it seems that no specific choice of these parameters can increase the honest symmetry, as we will discuss in section 5.

As it is, (2.10) implies altogether $Z_2^5$ symmetry on $K_0$:

$$\begin{aligned}
&\text{(i)} \quad Z_2(A): \quad x_i \to A_{ij}x_j, \quad y_i \to A_{ij}y_j \\
&\qquad\qquad A_{ij} = \mathrm{diag}(-1,1,1,1,1) \\
&\text{(ii)} \quad Z_2(B): \quad B = \mathrm{diag}(1,-1,1,1,1) \\
&\text{(iii)} \quad Z_2(C): \quad C = \mathrm{diag}(1,1,-1,1,1) \\
&\text{(iv)} \quad Z_2(D): \quad D = \mathrm{diag}(1,1,1,-1,1) \\
&\text{(v)} \quad Z_2(S): \quad S(x_i) = y_i, S(y_i) = x_i .
\end{aligned} \tag{4.1}$$

Notice that $x_4 \to -x_4$ symmetry is not independent; it is generated by -ABCD.

Since all these generators commute with each other and with $G_F$, they all survive down to K. Since $g_1$ and $g_2$ depend on the generators (4.1) through $g_1 = ABC$, $g_2 = ABD$ on $CP_4 \times CP_4$, we identify the honest symmetry of K as

$$G_H = \frac{Z_2(A) \times Z_2(B) \times Z_2(C) \times Z_2(D) \times Z_2(S)}{G_F = Z_2(g_1) \times Z_2(g_2)} \quad . \tag{4.2}$$

$G_H = Z_2^3$ is generated by A, B and S. The trivial embedding in E(6)

$U_A = U_B = U_S = 1$ keeps $G_H$ unbroken even after the flux breaking (of course, this requires $U_C = U_{g_1}, U_D = U_{g_2}$).

We now give the transformation properties of physical fields under A and B generators (the behaviour under swapping is obvious).

(i) $h_{21}$:

It is straightforward to reproduce the transformation properties of (2,1) fields in Table 2.

(ii) $h_{11}$:

We could use again Lefschetz fixed point theorems as given in (2.17); it would suffice to compute $\chi$(fixed points of A) and $\chi$(fixed points of B), since we already know $TrH_{21}(A)$, $TrH_{21}(B)$. However, this way we would miss the transformation properties of the fields under S. For this reason, and in order to have an independent check, one can employ the hyperplane version of the fixed point theorem. In simplest terms, this just means that we can ignore the mixed polynomial $P_3$ of (2.10) and use (2.17) as applied on each individual space $U \equiv (4\|22)$. In other words

$$[TrH_{11}(g) \text{ on } K] = 2\,[TrH_{11}(g) \text{ on } U] \quad , \tag{4.3}$$

where g is the transformation of interest (g stands for A, B here); and $TrH_{11}(g)$ on U is determined from

$$\sum_{p,q=0}^{2} (-1)^{p+q}\,[TrH_{pq}(g) \text{ on } U] = \chi(\text{fixed points of } g \text{ on } U) \ . \tag{4.4}$$

As before, the right hand side is the Euler characteristic of the fixed

submanifold of g. Since U is not a Calabi-Yau manifold ($c_1(U) \neq 0$) and $\chi_E(U)>0$, $h_{20}(U) = h_{10}(U) = 0$ and (4.4) reads

$$[\mathrm{TrH}_{11}(g) \text{ on } U] + 2 = \chi \text{ (fixed points of } g \text{ on } U) \ . \qquad (4.5)$$

Now, we would like to classify our physical fields in (3.11), so g will stand actually for the projections, such as $\frac{1}{2}(1+g_1)\frac{1}{2}(1+g_2)A$, etc. We introduce the notation

$$\begin{aligned}
\mathrm{TrH}_{11}(g(\bar{n})) &= \frac{1}{4}\,[\mathrm{TrH}_{11}(g) + \mathrm{TrH}_{11}(g_1 g) + \mathrm{TrH}_{11}(g_2 g) + \mathrm{TrH}_{11}(g_1 g_2 g)] \\
\mathrm{TrH}_{11}(g(\bar{Q}_L)) &= \frac{1}{4}\,[\mathrm{TrH}_{11}(g) - \mathrm{TrH}_{11}(g_1 g) + \mathrm{TrH}_{11}(g_2 g) - \mathrm{TrH}_{11}(g_1 g_2 g)] \\
\mathrm{TrH}_{11}(g(\bar{Q}_R)) &= \frac{1}{4}\,[\mathrm{TrH}_{11}(g) + \mathrm{TrH}_{11}(g_1 g) - \mathrm{TrH}_{11}(g_2 g) - \mathrm{TrH}_{11}(g_1 g_2 g)] \\
\mathrm{TrH}_{11}(g(\bar{\phi})) &= \frac{1}{4}\,[\mathrm{TrH}_{11}(g) - \mathrm{TrH}_{11}(g_1 g) - \mathrm{TrH}_{11}(g_2 g) + \mathrm{TrH}_{11}(g_1 g_2 g)] \ ,
\end{aligned} \qquad (4.6)$$

where $g = A,B$ and the reader should recall that $\bar{D}$ and $\bar{D}^c$ transform as $\bar{n},\bar{\psi}_L$ as $\bar{Q}_L,\bar{\psi}_R$ as $\bar{Q}_R$.

Let us look at $g = A$ first. The fixed manifold is $(3\|22) =$ torus $T_2$, and so $\chi$(fixed point of A on U) = 0 or

$$\mathrm{TrH}_{11}(A) \text{ on } U = -2 \ . \qquad (4.7)$$

Similarly,

$$\begin{aligned}
\mathrm{TrH}_{11}(gA) \text{ on } U &= 2 \\
\mathrm{TrH}_{11}(g_2 A) \text{ on } U &= 2 \\
\mathrm{TrH}_{11}(g_1 g_2 A) \text{ on } U &= 2 \ ,
\end{aligned} \qquad (4.8)$$

since on U above elements have four fixed points. When all the dust settles, on U one gets

$$\mathrm{Tr}H_{11}(A(\bar{n})) = \mathrm{Tr}H_{11}(B(\bar{n})) = 1$$

$$\mathrm{Tr}H_{11}(AB(\bar{n})) = -1, \quad \mathrm{Tr}H_{11}(1(\bar{n})) = 3 \tag{4.9}$$

and

$$\mathrm{Tr}H_{11}(A(\bar{\phi})) = \mathrm{Tr}H_{11}(B(\bar{\phi})) = -1$$

$$\mathrm{Tr}H_{11}(AB(\bar{\phi})) = \mathrm{Tr}H_{11}(B(\bar{\phi})) = 1 \ , \tag{4.10}$$

with

$$\mathrm{Tr}H_{11}(g(\bar{Q}_L)) = \mathrm{Tr}H_{11}(g(\bar{Q}_R)) = \mathrm{Tr}H_{11}(g(\bar{\phi})) \quad . \tag{4.11}$$

If we denote $f=(Q_L,Q_R,\psi_L,\psi_R,\phi)$ and $F=(n,D,D^c)$, then the number $c_i$ of $\bar{f}$ and $\bar{F}$ fields in each of the representations $r_i$ in Table 2 is on U:

$$c_1(\bar{F}) = 1, \quad c_1(\bar{f}) = 0 \qquad c_3(\bar{F}) = 1, \quad c_3(\bar{f}) = 0$$

$$c_2(\bar{F}) = 1, \quad c_2(\bar{f}) = 0 \qquad c_4(\bar{F}) = 1, \quad c_4(\bar{f}) = 1 \ . \tag{4.12}$$

Recall that on K $h_{11}$ consists of 6 $\bar{F}$ and 2 $\bar{f}$ fields—see (3.10). From (3.12), we learn that in each $U=(3\|22)$ submanifold there are $3\bar{F}$'s and $1\bar{f}$ related by the swapping symmetry. In summary, we can name the $\bar{F}$'s and $\bar{f}$'s in the following manner

$$\bar{F}_1 \epsilon r_1 < \underline{S} > \bar{F}_4 \epsilon r_1$$

$$\bar{F}_2 \epsilon r_2 < \underline{S} > \bar{F}_5 \epsilon r_2$$

$$\bar{F}_3 \epsilon r_3 < \underline{S} > \bar{F}_6 \epsilon r_3 \tag{4.13}$$

and

$$\bar{f}_1 \epsilon r_4 < \underline{S} > \bar{f}_2 \epsilon r_4 \quad . \tag{4.14}$$

This completes the study of predominantly mathematical properties of

our manifold. We now have all the quark and lepton fields which have survived the compactification to d = 4 and the associated topological symmetry breaking via Wilson flux lines. We also know all the symmetries of K and the transformation properties of the fields under them. There is still a large intermediate gauge symmetry based on $SU(2)_L$ x $SU(2)_R$ x $SU(4)_C$ group. Next step is to discuss the phenomenological consequences for the low energy weak interaction phenomena.

## V. SUMMARY AND OUTLOOK

We have managed to construct a new four generation Calabi-Yau manifold with two main characteristics:

(i) $h_{21} = 10$, $h_{11} = 6$ and so this manifold does not suffer from the usual problem associated with $h_{11} = 1$ as previous examples, such as $(4\|5)$ and $(7\|2222)$. This was our main motivation.

(ii) The nontrivial and suggestive embedding of our freely acting $Z_2 \times Z_2$ symmetry in E(6) leads to Pati-Salam intermediate symmetry. Even if the fourth generation may not be found soon, this still provides a nontrivial departure from the 3 generation Tian-Yau manifold. Of course, a careful phenomenological investigation must be performed before we make a case for either this or the Tian-Yau manifold; in particular one has to discuss the next stage of symmetry breaking and its impact on the low energy physics. If all goes well, one finally has to address the issue of Yukawa couplings, which requires in general large symmetries. Can we increase the honest symmetry $G_F$ discussed in section 4 by a specific choice of the $a_i$, $b_i$ and $c_i$ parameters? It seems not. One may even wonder if there is a simple choice of these parameters consistent with the conditions for transversality discussed in the Appendix. Here fortunately the answer is yes. A particular elegant and consistent complex structure of (2.10) is given by

$$a_k = e^{i\frac{2\pi}{5}k}, \quad c_k = a_k^* , \qquad (5.1)$$

$$k = 0,1,2,3,4 \quad .$$

This implies a $Z_5$ cyclic symmetry on $K_0$:

$$P: \quad x_i \to x_{i+1}, \quad y_i \to y_{i+1} , \tag{5.2}$$

with

$$P_1 \to P_1, \quad P_2 \to e^{-i\frac{2\pi}{5}} P_2, \quad P_3 \to e^{i\frac{2\pi}{5}} P_3 ,$$

$$P_4 \to e^{-i\frac{2\pi}{5}} P_4, \quad P_5 \to P_5 , \tag{5.3}$$

so that new polynomials still vanish. For this to be an honest symmetry on K, we need

$$P^{-1} g_1 P \in G_F . \tag{5.4}$$

It is easily verified that

$$P^{-1} g_1 P = g_1 g_2 \in G_F ,$$

but

$$P^{-1} g_1 g_2 P = \mathrm{diag}(1,-1,1,1,-1) \notin G_F . \tag{5.5}$$

Of course, (5.1) is still interesting, since P symmetry may be useful in evaluating Yukawa couplings. It is actually the largest possible symmetry on $K_0$ consistent with the transversality conditions derived in the Appendix.

It may be worth commenting that we cannot enlarge $G_F$ by including the element above, since one can easily see that it does not act freely on $K_0$ when multiplied by (say) $g_1 g_2$. In other words, in this way K

cannot be made into a two generation manifold.

We have tried hard to achieve the above, motivated by the fact that $K_0$ satisfies the criteria of Aspinwall et al. to actually accommodate two light generations. Although we have failed, a more persistent reader may be encouraged to try, since we cannot prove that K is not a two generation manifold. This may not be a futile exercise, in view of the suggestion [24] that the extra generation (and its mirrors) may come from all the stuff in (3.11).

## APPENDIX

Here we show that the polynomials (2.10) are transverse for a generic choice of the coefficients $a_i$, $c_i$ and obtain the constraints on these coefficients. This proves that $K_0$ is a smooth manifold.

We need to check that $\Pi_{i=1}^{5} dP_i = dP_1 \wedge dP_2 \wedge dP_3 \wedge dP_4 \wedge dP_5$ does not vanish on $K_0$. From (2.10)

$$0 = \prod_{i=1}^{5} dP_i = A(x,y) \wedge B(y) + B(x) \wedge A(y,x) \ , \tag{A.1}$$

where

$$A(x,y) = \sum_{i,j,k=0}^{4} a_j c_k x_i x_j y_k dx_i \wedge dx_j \wedge dx_k \ ,$$

$$B(x) = \sum_{i,j=0}^{4} a_j x_i x_j dx_i \wedge dx_j \ . \tag{A.2}$$

Since they are linearly independent, each term in (A.1) vanishes separately. Furthermore, as long as

$$a_m - a_n \neq 0 \text{ for } m \neq n \ , \tag{A.3}$$

B's cannot vanish. Hence

$$A(x,y) = 0 = A(y,x) \ . \tag{A.4}$$

The first condition is a set of ten coupled equations

$$x_0x_1y_2(a_1-a_0)c_2-x_0x_2y_1(a_2-a_0)c_1+x_1x_2y_0(a_2-a_1)c_0 = 0 \quad /1/$$

$$x_0x_1y_3(a_1-a_0)c_3-x_0x_3y_1(a_3-a_0)c_1+x_1x_3y_0(a_3-a_1)c_0 = 0 \quad /2/$$

$$x_0x_1y_4(a_1-a_0)c_4-x_0x_4y_1(a_4-a_0)c_1+x_1x_4y_0(a_4-a_1)c_0 = 0 \quad /3/$$

$$x_0x_2y_3(a_2-a_0)c_3-x_0x_3y_2(a_3-a_0)c_2+x_2x_3y_0(a_3-a_2)c_0 = 0 \quad /4/$$

$$x_0x_2y_4(a_2-a_0)c_4-x_0x_4y_2(a_4-a_0)c_2+x_2x_4y_0(a_4-a_2)c_0 = 0 \quad /5/$$

$$x_0x_3y_4(a_3-a_0)c_4-x_0x_4y_3(a_4-a_0)c_3+x_3x_4y_0(a_4-a_3)c_0 = 0 \quad /6/$$

$$x_1x_2y_3(a_2-a_1)c_3-x_1x_3y_2(a_3-a_1)c_2+x_2x_3y_1(a_3-a_2)c_1 = 0 \quad /7/$$

$$x_1x_2y_4(a_2-a_1)c_4-x_1x_4y_2(a_4-a_1)c_2+x_2x_4y_1(a_4-a_2)c_1 = 0 \quad /8/$$

$$x_1x_3y_4(a_3-a_1)c_4-x_1x_4y_3(a_4-a_1)c_3+x_3x_4y_1(a_4-a_3)c_1 = 0 \quad /9/$$

$$x_2x_3y_4(a_3-a_2)c_4-x_2x_4y_3(a_4-a_2)c_3+x_3x_4y_2(a_4-a_3)c_2 = 0 \quad /10/ \quad . \tag{A.5}$$

The second condition is obtained from the above equations by the substitution x <-> y. We now show that (A.5) has no solution.

(i) Assume first all $x_i, y_i \neq 0$. Take the ratio of Eqs. /1/ and /2/, and the same ratio of their symmetric sisters

$$\frac{c_2}{c_3}\frac{y_2}{y_3} = \frac{x_2}{x_3}\frac{\left(a_2 - a_0\right)c_1x_0y_1 - \left(a_2 - a_1\right)c_0x_1y_0}{\left(a_3 - a_0\right)c_1x_0y_1 - \left(a_3 - a_1\right)c_0x_1y_0}$$

$$\frac{c_2}{c_3}\frac{x_2}{x_3} = \frac{y_2}{y_3}\frac{\left(a_2 - a_0\right)c_1x_1y_0 - \left(a_2 - a_1\right)c_0x_0y_1}{\left(a_3 - a_0\right)c_1x_1y_0 - \left(a_3 - a_1\right)c_0x_0y_1} \quad . \tag{A.6}$$

Define $u \equiv \frac{x_0y_1}{x_1y_0}$; (A.6) gives a quadratic equation for u:

$$u^2 - Bu + 1 = 0 \quad , \tag{A.7}$$

where

$$B = \frac{c_3^2\left[(a_2 - a_0)^2 c_1^2 + (a_2 - a_1)^2 c_0^2\right] - c_2^2\left[(a_3 - a_0)^2 c_1^2 + (a_3 - a_1)^2 c_0^2\right]}{c_0 c_1\left[c_3^2(a_2 - a_0)(a_2 - a_1) - c_2^2(a_3 - a_0)(a_3 - a_1)\right]} \quad . \tag{A.8}$$

Similarly, for $\frac{/1/}{/3/}$ we get another equation for u, with

$$B' = B(a_3 \to a_4; c_3 \to c_4) \quad . \tag{A.9}$$

In order for (A.7)-(A.9) to have no solution an additional condition emerges:

$$B \neq B' \quad . \tag{A.10}$$

Strictly speaking, it is sufficient that any of the corresponding conditions for ratios such as $\frac{x_1 y_3}{x_3 y_1}$ , $\frac{x_1 y_4}{x_4 y_1}$ ,..., etc. is satisfied.

ii) Next, let us assume that only one x coordinate vanishes, say $x_0 = 0$. From /1/, $y_0 = 0$, too, which means that we are searching for the possibility $x_0 = y_0 = 0$ and the rest $x_i$, $y_i \neq 0$. Conditions /1/,...,/6/ then vanish identically. As in the case i), we can still determine (but not over-determine) ratios $\frac{x_1 y_2}{x_2 y_1}$ , $\frac{x_1 y_3}{x_3 y_1}$ , $\frac{x_1 y_4}{x_4 y_1}$ . We write them as

$$\frac{y_2}{y_1} = \alpha\frac{x_2}{x_i} \; ; \quad \frac{y_3}{y_1} = \beta\frac{x_3}{x_1} \; ; \quad \frac{y_4}{y_1} = \gamma\frac{x_4}{x_1} \; ;$$

$$\alpha,\beta,\gamma = \frac{B_{1,2,3} \pm \left(B^2_{1,2,3}-4\right)^{1/2}}{2} \quad , \tag{A.11}$$

where

$$B_1 = B(a_i \rightarrow a_{i+1}, c_i \rightarrow c_{i+1})$$

$$B_2 = B(a_0 \rightarrow a_1 \rightarrow a_3 \rightarrow a_4; \quad c_0 \rightarrow c_1 \rightarrow c_3 \rightarrow c_4)$$

$$B_3 = B(a_0 \rightarrow a_1 \rightarrow a_4; \quad c_0 \rightarrow c_1 \rightarrow c_4) \quad . \tag{A.12}$$

From $P_i = 0$ $(i=1,\ldots,5)$, we get then

$$\begin{aligned} x_1^2 + x_2^2 + x_3^2 + x_4^2 &= 0 \\ a_1x_1^2 + a_2x_2^2 + a_3x_3^2 + a_4x_4^2 &= 0 \\ c_1x_1^2 + c_2\alpha x_2^2 + c_3\beta x_3^2 + c_4\gamma x_4^2 &= 0 \\ a_1x_1^2 + a_2\alpha^2x_2^2 + a_3\beta^2x_3^2 + a_4\gamma^2x_4^2 &= 0 \\ x_1^2 + \alpha^2x_2^2 + \beta^2x_3^2 + \gamma^2x_4^2 &= 0 \quad . \end{aligned} \tag{A.13}$$

But $x_1 \neq 0$ by assumption and on $CP_4$ we can always scale it to be 1. This implies 5 equations with 3 unknowns ($x_2$, $x_3$, $x_4$), which in general is expected to have no solution. To be more specific, by subtracting the first equation from the rest in (A.13), we derive four homogeneous equations:

$$(a_2-a_1)x_2^2 + (a_3-a_1)x_3^2 + (a_4-a_1)x_4^2 = 0$$

$$(c_2\alpha-c_1)x_2^2 + (c_3\beta-c_1)x_3^2 + (c_4\gamma-c_1)x_4^2 = 0$$

$$(a_2\alpha^2-a_1)x_2^2 + (a_3\beta^2-a_1)x_3^2 + (a_4\gamma^2-a_1)x_4^2 = 0$$

$$(\alpha^2-1)x_2^2 + (\beta^2-1)x_3^2 + (\gamma^2-1)x_4^2 = 0 \quad . \tag{A.14}$$

Since in this case we assumed $x_2$, $x_3$, $x_4 \neq 0$, as long as any one of the 3 x 3 subdeterminants of the above system is nonvanishing, there will be no solution to (A.14).

Although it is not illuminating to write down all conditions, the reader should be aware of the analogous demands in order not to have any of the other $x_i = y_i = 0$ possibilities. Needless to say, all of them must be verified when a specific set of complex structures is chosen.

iii) Finally, we consider the case $x_0 = y_0 = 0$ and say $x_1 = 0$. From (A.5) then either $x_2 = 0$ or $y_1 = 0$. Now, $P_1 = P_2 = 0$ and the condition (A.3) imply immediately no solution with $x_2 = 0$. In other words, case $x_0 = y_0 = x_1 = y_1$ is the last one we have to analyze.

$P_i = 0$ then gives a set of equations completely analogous to (2.13). Recall the conditions (2.14) (and use (A.3))

$$Q_{012} = c_0(a_1 - a_2) \pm c_1(a_2 - a_0) \pm c_2(a_0-a_1) \neq 0 \quad . \tag{A.15}$$

In complete analogy, we need (in obvious notation)

$$Q_{234} \neq 0 \quad . \tag{A.16}$$

Again, to eliminate all the solutions with two x's and y's vanishing we require altogether ten conditions $Q_{rst} \neq 0$, for any $r \neq s \neq t$. Notice

that these conditions guarantee the absence of fixed points for the dividing $Z_2 \times Z_2$ symmetry.

References


1. L. Boltzmann, Ber. Wien. Akad. **66**, 275 (1872).
2. S. Chandrasekhar, **Radiative Transfer** (Dover, New York, 1960).
3. K. M. Case and P. F. Zweifel, **Linear Transport Theory** (Addison-Wesley, Reading, Mass., 1967).
4. E. W. Larsen and G. W. Habetler, Comm. Pure Appl. Math. **26**, 525 (1973).
5. R. J. Hangelbroek, TTSP **5**, 1 (1976).
6. W. Greenberg and P. F. Zweifel, J. of Math. Phys. **17**, 163 (1976).
7. W. Greenberg and P. F. Zweifel, TTSP **5**, 219 (1976).
8. P. F. Zweifel, TTSP **11**, 183 (1983).
9. W. Greenberg, C. V. M. van der Mee and P. F. Zweifel, Integral Equations and Operator Theory **7**, 60 (1984).
10. J. H. Ferziger and H. G. Kaper, **Mathematical Theory of Transport Processes in Gases** (North Holland, Amsterdam, 1972).
11. P. F. Zweifel, **Reactor Physics** (McGraw-Hill, New York, 1973).
12. C. Cercignani, **Theory and Application of the Boltzmann Equation** (Elsevier, New York, 1975).
13. M. M. R. Williams, **The Slowing Down and Thermalization of Neutrons** (North Holland, Amsterdam, 1966).
14. J. H. Ferziger and P. F. Zweifel, **The Theory of Neutron Slowing Down in Nuclear Reactors** (MIT Press, Cambridge, 1966).
15. W. Greenberg, C. van der Mee, V. Protopopescu, **Boundary Value Problems in Abstract Kinetic Theory** (Birkhauser Verlag, Basel, 1987).
16. A. Alberigi-Quaranta et al., Phys. Rev. **177**, 2118 (1969).
17. S. S. Gershtein and L. I. Ponomarev in **Muon Physics 3** (edited by

V. W. Hughes and C. S. Wu, Academic Press, New York, 1975).

18. F. C. Frank, Nature **160**, 525 (1947).

19. L .W. Alvarez et al., Phys. Rev. **105**, 1127 (1957).

20. H. Bossy et al., Phys. Rev. Lett. **55**, 1870 (1985).

21. J. S. Cohen, Phys. Rev. Lett. **58**, 1407 (1987).

22. M. Leon and J. S. Cohen, Phys. Rev. A **31**, 2680 (1985).

23. M. Leon, Phys. Rev. Lett. **52**, 605 (1984).

24. J. Rafelski and S. E. Jones, Scientific American, July 1987.

25. R. Siegel, private correspondence.

26. B. D. Ganapol and L. M. Grossman, Nuclear Sci. and Eng. **52**, 454 (1973).

27. B. D. Ganapol, P. W. McKenty and K. L. Peddicord, Nuclear Sci. and Eng. **64**, 317 (1977).

28. L. I. Schiff, **Quantum Mechanics** (McGraw-Hill, New York, 1949).

29. P. F. Zweifel and H. Hurwitz Jr., J. Appl. Phys. **25**, 1241 (1954).

30. A. Rahman, J. Nucl. Energy A **13**, 128 (1961).

31. E. P. Wigner and J. E. Wilkins, AECD 2275 (1944).

32. A. M. L. Messiah, Phys. Rev. **84**, 204 (1951).

33. W. H. Press, B. P. Flannery, S. A. Teukolsky and W. T. Vetterling, **Numerical Recipes** (Cambridge University Press, Cambridge, 1986).

34. G. Henneke, private communication.

35. L. I. Ponomarev, L. N. Somov and M. I. Faifman, Sov. J. Nucl. Phys. **29**, 67 (1979).

36. M. Bubak and M. P. Faifman, E4-87-464, Joint Institute for Nuclear Research, Dubna, 1987.

37. M. M. Levine, K. E. Roach, D. B. Wehmeyer and P. F. Zweifel, Nuclear

Sci. and Eng. **7**, 14 (1960).

38. T. J. Krieger and P. F. Zweifel, Nuclear, Sci. and Eng. **5**, 21 (1959).
39. P. F. Zweifel and J. H. Ferziger, Nuclear Sci. and Eng. **10**, 357 (1961).
40. H. Hurwitz, Jr. and P. F. Zweifel, J. Applied Phys. **26**, 923 (1955).
41. G. Goertzel and E. Greuling, Nuclear Sci. and Eng. **7**, 69 (1960).

PART II:

1. M. Green, J. Schwarz and E. Witten, **Superstring Theory**, Cambridge Univ. Press, 1987, is a comprehensive review of the subject.
2. See ref. 1, volume II, Chapters 12-16. For an excellent shorter review, see P. Candelas, Univ. of Texas preprint UTTG-21-87 (1987). For even shorter (telegraphic) review, see G. Horowitz, Santa Barbara preprint (1985).
3. P. Candelas, A. Dale, C. Lütken and R. Schimmrigk, Univ. of Texas preprints UTTG-10 and 11-87 (1987); P. Aspinwall, B. Greene, K. Kirklin and P. Miron, Oxford Univ. preprint 26/87 (1987).
4. P. Candelas, G. Horowitz, A. Strominger and E. Witten, Nucl. Phys. **B258**, 46 (1985).
5. G. Tian and S. T. Yau, in **Symposium on Anomalies, Geometry and Topology**, ed. W. Bardeen and A. White, World Scientific, Singapore (1985); page 395.
6. B. Greene, K. Kirklin, P. Miron and G. G. Ross, Nucl. Phys. **B278**, 667 (1986); **ibid 292**, 606 (1987); Phys. Lett. **B180**, 69 (1986).
7. S. Kalara and R. N. Mohapatra, Phys. Rev. **D36**, 3474 (1987).

8. S. Kalara, P. K. Mohapatra and R. N. Mohapatra, Univ. of Maryland preprint (to appear in Phys. Rev. D). G. Lazarides and Q. Shafi, Phys. Lett. B (to be published). E. Rusjan and G. Senjanović, Virginia Tech preprint (1988).

9. T. Hübsch, Comm. Math. Phys. **108**, 291 (1987).

10. Y. Hosotani, Phys. Lett. **129B**, 193 (1983).

11. We have been informed by Tristan Hübsch of the unpublished work of Candelas, Lüthens and Schimmrigk which claims about 60 candidates.

12. The (5‖33) manifold, contrary to the claim of Strominger and Witten, Comm. Math. Phys. **101**, 341 (1985) has fixed points (which is not a torus); see D. Chang, P. Pal, E. R. and G.S., unpublished.

13. S. Kalara and R. N. Mohapatra, Z. Phys. **C37**, 395 (1988).

14. This is a Calabi-Yau manifold, since the sum in each row is one plus the dimension of the corresponding $CP_n$ factor (n = 4 here); see Candelas, ref. 2 and references therein.

15. Greene et al., the first of ref. 6.

16. See ref. 1, pages 428-429.

17. For a diagramatic analysis of when the deformation methods works, see T. Hübsch and P. Green, Comm. Math. Phys. **113**, 505 (1987).

18. P. Candelas, Univ. of Texas preprint UTTG-50-87 (1988).

19. Lefschetz theorem is summarized in ref. 15.

20. For a nice expose of this technique, see M. Goodman and E. Witten, Nucl. Phys. **B271**, 21 (1986). For the application to Tian-Yau manifold, see ref. 15.

21. See, for example J. Mathews and R. L. Walker, Benjamin Press (1970) - chapter 16.

22. J. C. Pati and A. Salam, Phys. Rev. **D10**, 275 (1974).

23. R. Slansky, Phys. Rep. **C79**, 1 (1981).

24. C. Albright and A. Kagan, Fermilab preprint (1988).

Table 1. We give here all the 28 deformations ($h_{21}$ forms) and their transformation properties under $G_F$. The corresponding physical fields are identified.

| Deformations | $g_1$ | $g_2$ | Representation | Fields |
|---|---|---|---|---|
| $x_0^2,\ y_0^2$ | 1 | 1 | | |
| $x_1^2,\ y_1^2$ | 1 | 1 | | |
| $x_0y_1,\ x_1y_0$ | 1 | 1 | | |
| $x_1y_1$ | 1 | 1 | R1 | $\begin{pmatrix} n \\ D,\ D^c \end{pmatrix}$ |
| $x_2y_2$ | 1 | 1 | | |
| $x_3y_3$ | 1 | 1 | | |
| $x_4y_4$ | 1 | 1 | | |
| $x_0y_2,\ x_2y_0$ | 1 | -1 | | |
| $x_1y_2,\ x_2y_1$ | 1 | -1 | R2 | $(Q_R,\ \Psi_R)$ |
| $x_3y_4,\ x_4y_3$ | 1 | -1 | | |
| $x_0y_3,\ x_3y_0$ | -1 | 1 | | |
| $x_1y_3,\ x_3y_1$ | -1 | 1 | R3 | $(Q_L,\ \Psi_L)$ |
| $x_2y_4,\ x_4y_2$ | -1 | 1 | | |
| $x_0y_4,\ x_4y_0$ | -1 | -1 | | |
| $x_1y_4,\ x_4y_1$ | -1 | -1 | R4 | $(\phi)$ |
| $x_2y_3,\ x_3y_2$ | -1 | -1 | | |

Table 2. Analogous to Table 1; it gives the transformation properties of our fields under the honest symmetry generated by A and B. The swapping symmetry acts horizontally.

| Deformations | A | B | Representation | Fields |
|---|---|---|---|---|
| $x_0^2,\ y_0^2$ | 1 | 1 | | |
| $x_1^2,\ y_1^2$ | 1 | 1 | | |
| $x_1y_1$ | 1 | 1 | | |
| $x_2y_2$ | 1 | 1 | r1 | $\left(\begin{matrix} n \\ D,\ D^c \end{matrix}\right)$ |
| $x_3y_3$ | 1 | 1 | | |
| $x_4y_4$ | 1 | 1 | | |
| $x_0y_1,\ x_1y_0$ | -1 | -1 | r4 | |
| $x_0y_2,\ x_2y_0$ | -1 | 1 | r3 | |
| $x_1y_2,\ x_2y_1$ | 1 | -1 | r2 | $(Q_R,\ \Psi_R)$ |
| $x_3y_4,\ x_4y_3$ | 1 | 1 | r1 | |
| $x_0y_3,\ x_3y_0$ | -1 | 1 | r3 | |
| $x_1y_3,\ x_3y_1$ | 1 | -1 | r2 | $(Q_L,\ \Psi_L)$ |
| $x_2y_4,\ x_4y_2$ | 1 | 1 | r1 | |
| $x_0y_4,\ x_4y_0$ | -1 | 1 | r3 | |
| $x_1y_4,\ x_4y_1$ | 1 | -1 | r2 | $(\phi)$ |
| $x_2y_3,\ x_3y_2$ | 1 | 1 | r1 | |

The two page vita has been removed from the scanned document. Page 1 of 2

The two page vita has been removed from the scanned document. Page 2 of 2